

Mechanical Antenna Beam Steering

Intruder Detection with Electromagnetic Waves

Rikke Udengaard

Bachelor of Engineering in Electronics, Spring 24

Fifth Semester Project





Electronics and IT
Aalborg University
www.aau.dk

AALBORG UNIVERSITY STUDENT REPORT

Title:

Mechanical Antenna Beam Steering

Theme:

Digital and Analogue Systems Interacting with the Environment

Project Period:

Spring Semester 2024

Participant(s):

Rikke Udengaard

Supervisor(s):

Rocio Rodriguez Cano
Jan H. Mikkelsen

Copies: 1**Page Numbers:** 56**Date of Completion:**

May 23, 2024

Abstract:

In this project two directional antennas, one fixed and one steerable, are employed to determine the direction of transmission in the horizontal plane and rotate to face that direction. To test the full system with and without a static intruder two identical horn antennas were used. Each antenna has a gain of 11.41 dB at $f = 4.75\text{ GHz}$ and 12.99 dB at $f = 5.65\text{ GHz}$. The results show that the maximum gain of the received signal at both frequencies is in the direction of the transmitter with reflections detected in directions of vertical surfaces in the measurement space, and that the maximum gain in the direction of the transmitter measured is higher without intruder. It is concluded that an intruder can be detected with the system when comparing with measurements without intruder and that the intruder affects the direction of the maximum gain measured in the environment.

The content of this report is freely available, but publication (with reference) may only be pursued due to agreement with the author.

Contents

Preface	vi
1 Introduction	1
2 Technical Analysis	3
2.1 Fundamentals of Antennas	3
2.1.1 Propagation In Free Space	3
2.1.2 Polarization	4
2.1.3 Radiation Characteristics	5
2.1.4 Friis' Transmission Equation	6
2.1.5 S-Parameters	7
2.2 Antenna Designs	9
2.3 Beam Steering Methods	12
2.3.1 Electrical Steering	12
2.3.2 Manual and Mechanical Steering	13
3 Requirement Specification	15
3.1 Delimitations	15
3.2 Functional Requirements	15
3.3 Technical Requirements	16
4 System Design	17
4.1 Antenna Design	17
4.2 Choice of Turntable	19
4.3 Choice of Vector Network Analyzer	19
4.4 Design of Software Control Program	19
4.4.1 Communication Interfaces	19
4.4.2 Concurrency	20
5 Implementation	21
5.1 Turntable Control	22
5.2 VNA Control	25

5.3	Main Control Flow	27
6	Measurement Results	31
6.1	Equipment	31
6.2	Procedure	32
6.3	Test Results	32
6.3.1	Straight Setup	33
6.3.2	Straight Setup With Intruder	34
6.3.3	Corner-To-Corner Setup	36
6.3.4	Corner-To-Corner Setup With Intruder	38
6.3.5	Perpendicular Antennas	40
6.4	Test Results Comparison	42
7	Discussion	45
8	Conclusion	47
	Bibliography	48
A	Source Code Link	50
B	Test of Antenna Characteristics	51
B.1	Test of Horn Antenna S-Parameters	51
B.1.1	Equipment	51
B.1.2	Procedure	51
B.1.3	Result	52
B.2	Test of Horn Antenna Radiation Pattern	52
B.2.1	Equipment	52
B.2.2	Procedure	53
B.2.3	Result	53

Preface

This project was developed by Rikke Udengaard in the Spring semester of 2024 at Department of Electronic System at Aalborg University. The theme of this 5th semester project is *Digital and Analogue Systems Interacting with the Environment*.

The project includes source code that is available on *Github*. The link to the *Github* repository can be found in appendix A while some of the source code is explained in the implementation chapter 5. The repository also contains the test result logs, which are also found in a condensed form in the accept test results in section 6.

The block diagrams used throughout this report have been generated with `app.diagrams.net`. *CST Studio* and *Matlab* have been used to generate data plots. If the figure is retrieved from a source, the source is listed in the figure caption.

Prefixes and units are written in accordance to the SI system of units. The bibliography is found after the main report and before the appendix. The references are numbered in alphabetical order according to the authors' surnames.

The author of this project would like to thank Kim Olesen for his assistance in the antenna lab at Aalborg University including measurements of the antenna. The author would also like to thank Rocio Rodriguez Cano for her active role as supervisor during the project.

Aalborg University, May 23, 2024

Rikke Udengaard
<rudeng20@student.aau.dk>

1 Introduction

Modern requirements for higher data speed from users all over the world has introduced new developments in antenna design for wireless communication, specifically with 5G and beyond. The data speeds needed for fast and immediate connectivity requires the antennas to transmit much more power than previously. This has given way for new antenna designs that have a higher gain and also higher directivity [15]. This also leaves areas where the antenna transmits very little and therefore areas where, if a user is positioned here, there will be very slow data rates. This can be mitigated by placing directive antennas in an array to ensure that the radiation pattern of the antennas covers the needed area. Doing this, the owner is sure that no matter where the user is in the needed area, there will always be signal, but it is also an expensive solution requiring a lot of hardware to cover larger physical areas. Another solution to mitigate the slow data rates in poorly covered areas is by controlling the beam of the antenna or antenna array and turning it to where the user is [15]. This means that fewer antennas could cover a larger area.

Some of the beam steering designs include use of antenna arrays and beam forming to multiply and magnify the electromagnetic waves. It is also possible with phased antenna arrays to steer the direction of the beam by changing the signal phase to each antenna element and thereby electronically controlling the direction of the beam towards the user [15]. In general, being able to steer the beam of a directive antenna in a direction ensures that a larger area of operation is possible although not concurrently.

Steering the beam towards the user makes it possible to establish a line-of-sight from the radio transmitter to the receiving user, which is the ideal transmission situation. Sometimes, however, the user might be moving or the line-of-sight path to the user might be broken by another object that interferes. This in itself leaves a new problem for the data transmission, but it can also be used to detect whether or not a physical object is intruding in the area between the receiver and the transmitter. Physical intruder detection systems are used to detect unauthorised entry into protected areas and usually include sensors and alarms of different kinds [12]. Intruder detection systems are used for many applications ranging from protect-

ing homes to military facilities and therefore exist in many configurations for the different application types and users.

This project has focus on beam steering of an antenna both for detecting a user and focusing the beam towards the user but also to detect an intrusion between a transmitter and a receiver.

2 Technical Analysis

The purpose of beam steering is to provide coverage in selected directions. This is enabled by having the main lobe of a radiation pattern of a directional antenna move to point towards the target of transmission and/or reception. Beam steering is purposeful for narrow directional beams. Beam steering can be performed using manual, mechanical or electronic with the main differences being method of implementation [20] [8]. This chapter explores the properties of antennas and beam steering methods, in order to understand antenna beam steering.

2.1 Fundamentals of Antennas

In order to develop a beam steering device for antennas it is necessary to understand antennas and their properties. Propagation, polarization, radiation characteristics are all properties of antennas that can vary based on the type of antenna.

2.1.1 Propagation In Free Space

Propagation of electromagnetic waves can be described with Maxwell's equations. In differential form they are as follows [19, p. 1]

$$\begin{aligned}\nabla \times \mathbf{E} &= -\frac{\partial}{\partial t} \mathbf{B} \\ \nabla \times \mathbf{H} &= \mathbf{J} + \frac{\partial}{\partial t} \mathbf{D} \\ \nabla \cdot \mathbf{B} &= 0 \\ \nabla \cdot \mathbf{D} &= \rho\end{aligned}\tag{2.1}$$

with \mathbf{E} being the electric field with unit $[V m^{-1}]$, \mathbf{B} being induction $[T]$, \mathbf{H} is magnetic field $[A m^{-1}]$, \mathbf{D} being dielectric displacement $[A s m^{-2}]$, \mathbf{J} being the current density $[A m^{-2}]$ and ρ being electric charge density $[C m^{-3}]$.

The electric field and the magnetic field are connected; the electric field is created by the magnetic field and vice versa. The electric field and the magnetic field in the spherical coordinate system (r, θ, ϕ, t) are illustrated on figure 2.1 below.

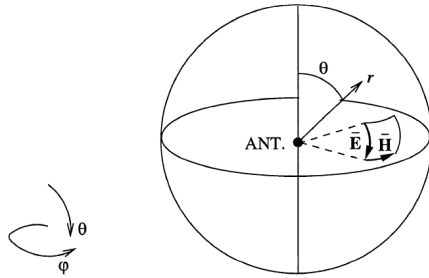


Figure 2.1: Electromagnetic propagation in the far field range around a small elemental antenna oriented along the z-axis visualised in the spherical coordinate system [6, p. 58].

As visualised on figure 2.1 the electric field only depends on the θ -component and the magnetic field only on the ϕ -component when in the far field. The vector \mathbf{r} is direction of the observation point. The length of \mathbf{r} is the distance to the observation point ie. distance between transmitting and receiving point [6, p. 59].

The Poynting vector describes the power density and direction of the electromagnetic flux and is the cross product of the electric and magnetic field

$$\mathbf{S} = \mathbf{E} \times \mathbf{H} \quad [\text{W m}^{-2}] \quad (2.2)$$

which points in the same direction as the wave propagation [19, p. 3].

Multipath propagation

the signal that reaches the receiving antenna can have travelled other paths than the direct line-of-sight path from the transmitter. This is because electromagnetic waves can reflect on surrounding surfaces, be changed by condition of the transmission medium or be Doppler shifted due to movement of the receiver, transmitter or other objects. The received signal is a summation of all input signals regardless of phase angles, phase shifts or directions and therefore the received signal might be distorted [16, pp. 1-2].

2.1.2 Polarization

Polarization describes the classification of the plane propagated wave, which is an electromagnetic wave that propagates with constant velocity in a specific direction. The direction of the propagation of the electromagnetic wave is always perpendicular to the direction of the electric field \mathbf{E} and both are perpendicular to the direction of the magnetic field \mathbf{H} . If the direction of the electric field is constant with time and position, the polarization of the propagated wave is classified as linear. If the direction of the electric field changes by rotating uniformly around the axis of the

propagated wave, the wave has circular polarization. The polarization of the receiving and transmitting antennas affects how the signal is detected. The signal is best received when the polarization of the receiver is the same as the polarization for the transmitter. Mismatch in polarization will result in less received power or more noise in the signal [14, p. 82-84].

Different antenna designs have different radiation patterns and polarization. Table 2.1 lists a number of different antenna designs and their polarization

Type	Polarization
Isotropic antenna	
Dipole antenna	Linear
Patch antenna	Linear, circular
Horn antenna	Linear, circular
Helical antenna	Circular

Table 2.1: Table showing polarization of some typical antenna designs [19, p. 11].

2.1.3 Radiation Characteristics

Electromagnetic waves propagate away from the source. Depending on the distance from the source, the electromagnetic waves can be found in the near field or the far field. The far field is mathematically described as the distance $r > R_2$, with R_2 defined as [19, p. 4]

$$R_2 = \frac{2D^2}{\lambda} \quad [\text{m}] \quad (2.3)$$

with D being the largest dimension of the antenna or antenna array and λ being the wavelength of the carrier frequency.

The radiation characteristics of an antenna can be described by the directivity, which is defined as the ratio of the maximum power density $S(\theta, \phi)_{max}$ radiated to the average power density $S(\theta, \phi)_{avg}$ radiated by an antenna. The directivity is unitless [14, p. 63]. An isotropic antenna is a theoretical antenna which radiates homogeneously in all directions, meaning that the magnitude of the power density vector \mathbf{S} at a distance vector \mathbf{r} is constant [19, p. 11]

$$D_{iso}(\theta, \phi) = \left| \frac{S(\theta, \phi)_{max}}{S(\theta, \phi)_{avg}} \right| = 1 \quad (2.4)$$

It is this theoretical isotropic radiator that the gain of antennas are in respect to. The directivity does not depend on the distance, r , in the far field, meaning that at the receiver, the relation $r \gg R_2$ is assumed. The directivity can then be described by [19, p. 10]

$$D(\theta, \phi) = \frac{S(\theta, \phi)_{max}}{S(\theta, \phi)_{avg}} \quad (2.5)$$

The total radiated power P_r is found by the surface integral of the power density. Assuming a spherical surface, the total radiated power is described as [23, p. 1-9]

$$P_r = \int_0^{2\pi} \int_0^\pi S(\theta, \phi) r^2 \sin \theta d\theta d\phi \quad [\text{W}] \quad (2.6)$$

The average radiated power over every direction in the sphere is given by [23, p. 1-9]

$$P_{avg} = \frac{P_r}{4\pi r^2} \quad [\text{W m}^{-2}] \quad (2.7)$$

Replacing the average power density $S(\theta, \phi)_{avg}$ in equation 2.5 with the average radiated power, the directivity of an antenna $D(\theta, \phi)$ can be defined as [19, p. 10]

$$D(\theta, \phi) = 4\pi r^2 \frac{S(\theta, \phi)_{max}}{P_r} \quad (2.8)$$

with $S(\theta, \phi)_{max}$ being the maximum power density and P_r being the total radiated power of the antenna.

The power of the source $P_{s,t}$ to a transmitting antenna might not equal the radiated power $P_{r,t}$ due to power loss $p_{l,t}$. Power loss can happen because of reflection loss in the input medium, conductor loss and dielectric loss. The efficiency of the transmitting antenna η is described as the ratio of the radiated power to the sourced power

$$\eta = \frac{P_{r,t}}{P_{s,t}} = \frac{P_{r,t}}{P_{r,t} + P_{l,t}} \quad (2.9)$$

The gain $G(\theta, \phi)$ of the antenna is the effective directivity, meaning how well the receiving or transmitting antenna is able to convert either electromagnetic waves or power into the other. The gain of a transmitting antenna can be calculated as [19, p. 10]

$$G_t(\theta, \phi) = \eta D_t(\theta, \phi) = 4\pi r^2 \frac{S(\theta, \phi)_{max}}{P_{s,t}} \quad (2.10)$$

or expressed in decibel with respect to the isotropic radiator [19, p. 10] [23, pp. 1.8-1.10].

$$G_{dBt} = 10 \log_{10}(G) \quad [\text{dB}] \quad (2.11)$$

2.1.4 Friis' Transmission Equation

The Friis transmission equation explains how the received power at a receiver is related to the power of the transmitter. The receiver antenna receives energy from the transmitting antenna and the effectiveness of this is described as the effective area $A_r(\theta, \phi)$ assuming that the antenna is placed in the origin of the spherical

coordinate system. If the antenna has the property of reciprocity, the effective area and the gain of the receiver antenna is related by [23, p. 1.10]

$$A_r(\theta, \phi) = \frac{\lambda^2}{4\pi} G_r(\theta, \phi) \quad [\text{m}^2] \quad (2.12)$$

If the gain of the transmitting antenna, G_t , is in the direction of the receiver antenna then the angular dependencies of the antenna properties can be suppressed. The power of the receiving antenna is equal to the power density $S(\theta, \phi)$ multiplied by the effective area of the receiver antenna A_r , expressed as

$$P_r = S_t A_r \quad [\text{W}] \quad (2.13)$$

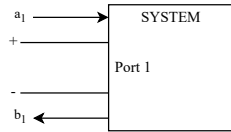
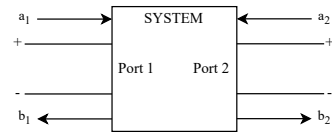
As previously mentioned the directivity of an antenna does not depend on the distance r from the antenna, and likewise so with the power density S_t , so the value of S_t is equal regardless of the distance from the antenna in the far field with respects to the angular dependencies. Substituting S_t and A_r in equation 2.13 for S_t isolated in equation 2.10 and A_r from equation 2.12 yields

$$\begin{aligned} P_r &= \frac{G_t P_t}{4\pi r^2} \frac{\lambda^2 G_r}{4\pi} \\ &= G_t G_r P_t \left(\frac{\lambda}{4\pi r} \right)^2 \end{aligned} \quad [\text{W}] \quad (2.14)$$

This is referred to as Friis' transmission equation [23, pp. 1.10-1.11]. The radiation characteristics of an antenna in the far field is called the antenna radiation pattern and will look different depending on the design of the antenna. The radiation pattern is dependent on the angular properties θ and ϕ and is usually visualised in a plane parallel to the electric field and called an **E** plane pattern or elevation plane pattern, or parallel to the magnetic field and called a **H** plane pattern or Azimuth plane pattern [14, p. 79-80][19, p. 13-14].

2.1.5 S-Parameters

S-parameters are used to describe the input and output relationship of a system's ports at microwave frequency [21]. S-parameters are used because voltages and currents can be difficult to measure directly in the microwave frequency spectrum. S-parameters describe a network in waves instead of voltages and currents [18]. S-parameters can be used to describe an n -port, $n \geq 1$, system and are dependent on frequency [21]. Some typical systems are one-port and two-port systems, visualised in figures 2.2 and 2.3.

**Figure 2.2:** One-port system.**Figure 2.3:** Two-port system.

The parameters a and b represent the waves flowing in and out of the system and they represent linear combinations of the voltages and currents at the ports [18]. Looking at a two-port system, such as a system with a receiver antenna and transmitter antenna, the S-parameter matrix looks as follows:

$$\begin{bmatrix} b_1 \\ b_2 \end{bmatrix} = \begin{bmatrix} s_{11} & s_{12} \\ s_{21} & s_{22} \end{bmatrix} \begin{bmatrix} a_1 \\ a_2 \end{bmatrix} \quad (2.15)$$

The S-parameters represent different information about the system as table 2.2 illustrates.

Parameter	Description
S_{11}	$S_{11} = \frac{b_1}{a_1}$. Forward reflection coefficient. Describes the input return loss Γ i.e. what is reflected from the port rather than radiated or absorbed.
S_{12}	$S_{12} = \frac{b_1}{a_2}$. Reverse transmission coefficient i.e. how much is transmitted from port 2 to port 1.
S_{21}	$S_{21} = \frac{b_2}{a_1}$. The forward transmission coefficient i.e. how much is transmitted from port 1 to port 2.
S_{22}	$S_{22} = \frac{b_2}{a_2}$. Reverse reflection coefficient i.e. output matching.

Table 2.2: Explanation of S-parameters [21].

Ideally, an electrical load is designed to have the least possible input return loss. This means the power transfer is maximised or the signal reflection is minimised, depending on the use case. Minimal reflection is achieved when the complex output impedance is equal to the complex input impedance and maximum power transfer is achieved when the complex output impedance is equal to the complex conjugate of the input impedance. If the input impedance of an electrical load is denoted Z_L and the characteristic output impedance of a signal source is denoted Z_0 [21][18], the return loss can be calculated as

$$\Gamma = \frac{Z_L - Z_0}{Z_L + Z_0} \quad (2.16)$$

Using the reflection coefficient the output flow at port one of a system is equal to $b_1 = \Gamma a_1$ [18]. S_{11} and the reflection coefficient Γ are related as follows:

$$S_{11} = 20 \log_{10} (|\Gamma|) \quad [\text{dB}] \quad (2.17)$$

2.2 Antenna Designs

The design of the antenna affects the radiation characteristics, the bandwidth and the range of frequencies at which the antenna is able to transmit or receive at [14, p. 76]. Bandwidth is the range of frequencies where the antenna is expected to operate in the wanted manner. There are several criterias that can be used to decide on the bandwidth for an antenna, for example the range where the reflection coefficient is less than a specified value or when the polarization fits a certain shape. The antenna design can also be designed to operate with a given bandwidth. The radiation pattern of an antenna varies with the frequency but the general shape is primarily decided by the design of the antenna [3]. The antenna types described in table 2.1 are some typical design types along with the isotropic antenna which is a theoretical antenna [19, p. 11].

A center-driven dipole antenna is two wires or rods pointing at the opposite direction of each other, for example towards positive and negative z in the spherical coordinate system. In the Azimuth plane the radiation pattern is a circle centered at the centre of the dipole antenna, whereas in the elevation plane, the radiation pattern is two ears extending from the centre to either side (see figure 2.4) [19, pp. 12-14]. The figure 2.4 shows a typical radiation pattern for a one-wavelength dipole antenna. As seen, the dipole antenna has a uniform pattern. Increasing the length of the dipole can increase the directiveness. However, the length also affects the input impedance. The dipole antenna will always have linear polarization [4].

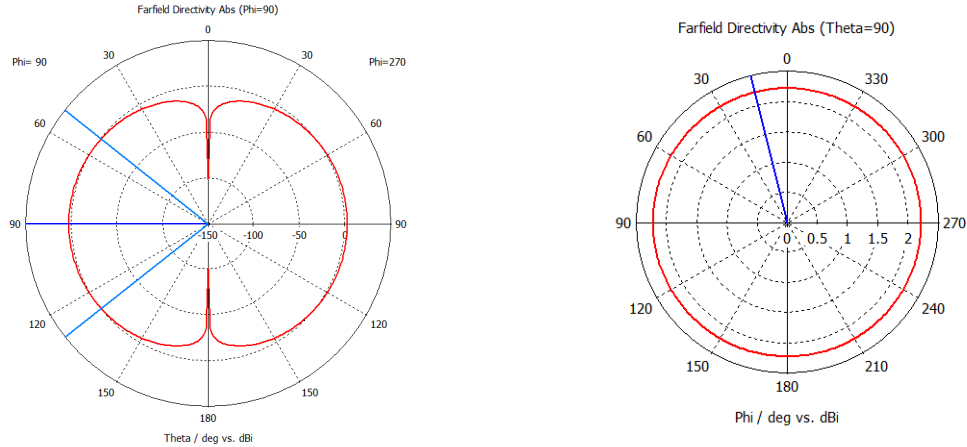


Figure 2.4: Dipole antenna radiation pattern. Figures generated with *CST Studio* dipole antenna example ($f = 2.4 \text{ GHz}$). The distance between the rods is 3.12 mm, the radius is 0.42 mm, the length is one half-wavelength or 62.5 mm.

A patch antenna is in its simplest form a piece of metal on top of a grounded surface. The metal can have different shape and size to accomodate different operating frequencies, bandwidths and gains. The feeding of the patch can also affect the antenna parameters such as the impedance match. The patch antenna is usually only used for microwave applications, because the flatness of the antenna allows it to fit into narrow areas, where the patch size must also be small. The operating frequencies depend on the size of the patch and vice versa. The patch antenna has lower efficiency than many other antenna design types, and a small bandwidth [23, p. 7.3]. The radiatation pattern depends, as in all cases, on the design of the patch, and can have a large variety of shape [23, p. 7.1-7.5]. An example can be seen in figure 2.5.

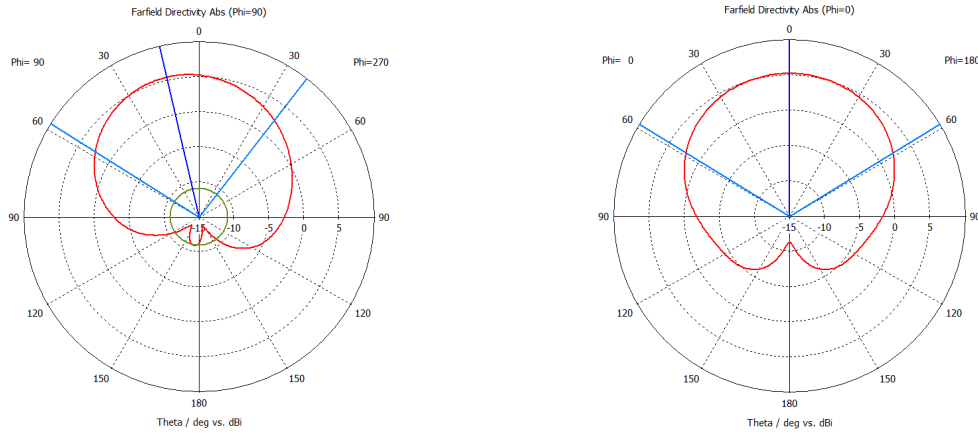


Figure 2.5: Patch antenna radiation pattern. Figures generated with *CST Studio* ($f = 2.4\text{ GHz}$). The dimensions are width 47 mm, height 30.2 mm, inset width 1.5 mm, inset height 7.16 mm, dielectric height 1.5 mm, substrate width and height 80 mm and transmission line length 2.98 mm.

Horn antennas come in many shapes and sizes which affect the radiation pattern and gain but common amongst the different designs is high beam directivity. A pyramidal, rectangular horn antenna is a common horn antenna, and has a fan-shaped radiation pattern. The gain can be calculated by knowing its dimensions and the beamwidth of the fan can be changed by varying the aperture dimensions. Horn antennas can be designed to cover both wide and narrow bandwidths, linear or circular polarization or to have a certain gain. Horn antennas are regarded as being able to fulfill many different applications [23, p. 14.1-14.3].

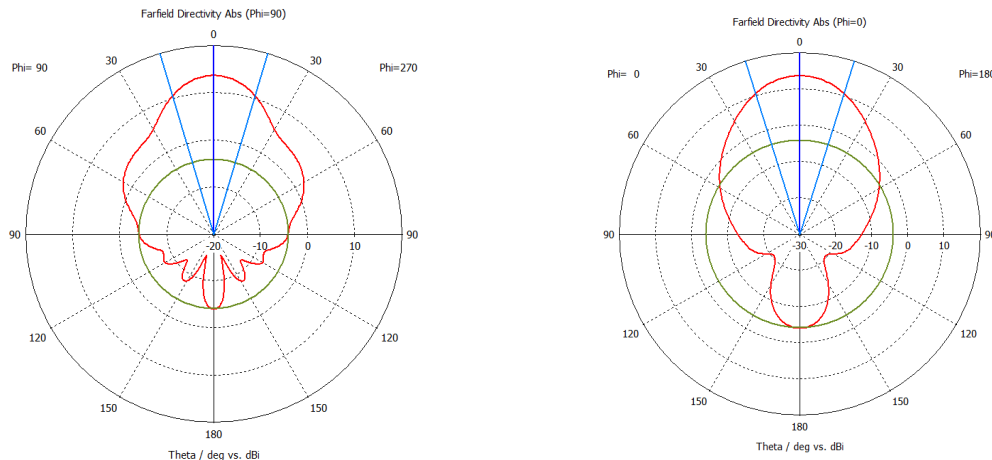


Figure 2.6: Horn antenna radiation pattern. Figures generated with *CST Studio* horn antenna example ($f = 2.4\text{ GHz}$). The antenna has an aperture width of 288 mm, aperture height of 211 mm, flare length 111 mm, metal thickness 0.62 mm, waveguide height 49 mm, waveguide length 125 mm and waveguide width 98 mm.

A helical antenna is one or several conductors in a helical shape connected to a ground plane and can be configured in many modes, the typical being *normal* or *axial* mode. Normal mode is achieved when the diameter of the helix is smaller than a wavelength and axial mode is when the circumference is close to the wavelength. A helix antenna has circular polarization in either right-hand or left-hand direction. A helix antenna has a wide spectrum for which impedance characteristics can be matched [23, p. 12.2].

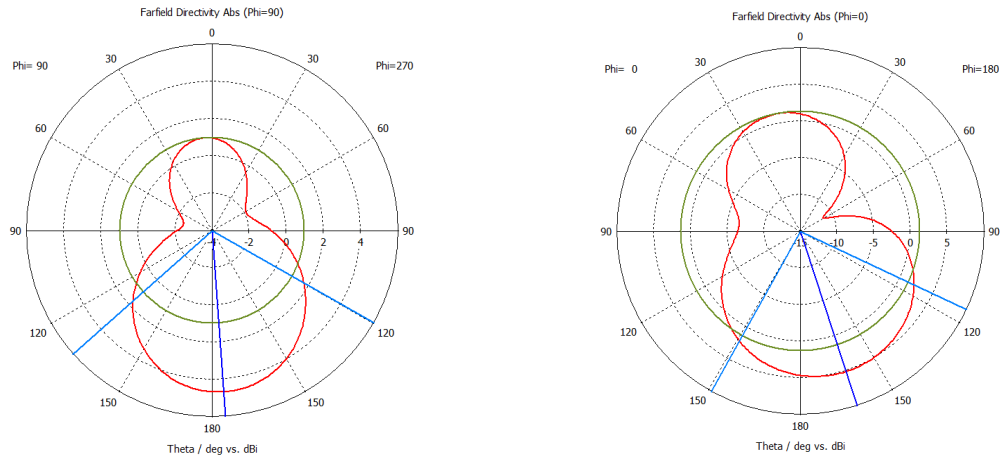


Figure 2.7: Helical antenna radiation pattern. Figures generated with *CST Studio* ($f = 2.4\text{ GHz}$). The coil dimensions are: height 67 mm, number of turns 9, clockwise orientation, segmentation angle $\phi = 14^\circ$, major and minor radius 4.77 mm.

2.3 Beam Steering Methods

Although the design of the antenna or antenna arrays decide the pattern of radiation, it is possible to modify this pattern or the direction of the pattern to achieve different directivities for other applications. The beam of the antenna can be steered in different directions for example, in order to cover a larger physical area with a single or few antennas or to focus a beam in a certain direction. Beam steering can be done manually, mechanically or electrically.

2.3.1 Electrical Steering

Electrical beam steering is the conventional steering method which builds upon beam forming methods. Beam forming means forming a single beam from a phased antenna array and controlling the shape and direction of this beam. Electrical beam steering does therefore not require changing the hardware or the setup but instead requires some form of control mechanism. Looking at a array of antennas, each element can be fed separately to be able to change the phase and

magnitude of each antenna element. Otherwise, if the antennas are fed with the same signal, the electromagnetic waves will combine and strengthen in the direction perpendicular to the antenna plane [15].

2.3.2 Manual and Mechanical Steering

Manual or mechanical steering differs from electrical steering in that it is not the beam that is steered but the antenna as a whole. For mechanical steering the antenna can be mounted on a rotating platform or arm that is controlled by a motor. There are several motor types that can rotate a platform or arm holding an antenna, for example a step motor or a servo motor.

A step motor has a rotor with two segments separated by a permanent magnet. The rotor segments have teeth which become poles of opposite polarity when the permanent magnet is axially magnetized. The rotor segments are also always skewed so that the teeth of one segment aligns with the gap between the teeth of the other rotor segment. The number of teeth determines the number of position steps around the center axis. The stator then generates a rotating magnetic field when the windings in the stator are supplied with current. The driver of the step motor controls the input current with PWM signals. The step motor usually works in an open loop configuration because of the design does not require feedback, however, overloading the motor might cause loss of synchronisation [22]. Figure 2.8 below shows a block diagram of an open loop configuration.



Figure 2.8: Open loop motor control block diagram [1].

Mathematically, the open loop configuration can be described by the open loop transfer function without feedback

$$\frac{Y(s)}{R(s)} = G(s)D(s)M(s) \quad (2.18)$$

Servo motors use a radially magnetized rotor, which means the number of poles determines the number of position steps around the center axis. This usually mean that a servo motor has less available positions than a step motor. The servo motor works like the step motor but an encoder is also used in the motor to give feedback to minimize error in the position [22]. The servo motor loop configuration can be seen on figure 2.9

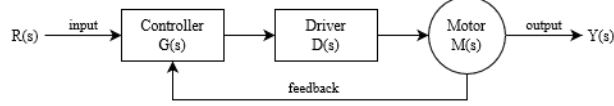


Figure 2.9: Closed loop motor control block diagram [1].

Mathematically, the closed loop configuration, with feedback denoted $H(s)$, can be described by the closed loop transfer function

$$\frac{Y(s)}{R(s)} = \frac{G(s)D(s)M(s)}{1 + G(s)D(s)M(s)H(s)} \quad (2.19)$$

The step and servo motor differ when it comes to the relationship between the speed and the torque characteristics. The step motor has high torque at low speeds which drops significantly as the speed increases. The servo motor has a flat torque up until high speeds. Usually, the step motor is most ideal for applications where discrete position accuracy and fast responsiveness is valued whereas the servo motor is most ideal in applications with high or varying loads [22].

3 Requirement Specification

The purpose of this project is to develop a setup where a receiving antenna is able to detect a transmitting antenna at an arbitrary point in space, redirect its beam towards that direction and to determine if it is possible to detect an intruder. Detection of electromagnetic waves can for example be used for intruder detection or can be further developed to include data transmission and thereby achieving higher throughput if the receiving antenna is able to locate and focus on the transmitting antenna.

Concluding on these two scenarios, it is required that the receiving antenna must be able to be controlled ie. steered in any direction and the electromagnetic radiation in the area must be measured.

3.1 Delimitations

The setup developed in this project is only designed to work in a two-dimensional, horizontal plane and also cover the 3 dB bandwidth in the elevation plane. Moreover, the choice of antenna will affect the discrete measurement points in the plane because of how the 3dB bandwidth will limit the accuracy of measurements. The project will focus on beam steering with mechanical turning, because electrical steering is outside the scope and requirements of the project.

3.2 Functional Requirements

The following table 3.1 outlines the functional requirements. The requirements in this section describe the functionality of the setup.

ID	Requirement	Traceability
F.1	Mechanically controlled turning along azimuth angle ϕ	Chapter 3 introduction, section 3.1
F.2	Data reading of electromagnetic radiation in the measurement space	Chapter 3 introduction, section 3.1
F.3	Controlled test environmental variables	Section 3.1
F.4	Automatic control of turning and measuring	Necessary to be able to reproduce test

Table 3.1: Table of functional requirements.

3.3 Technical Requirements

The table 3.2 below outlines the technical requirements. The requirements in this section describe the technical needs of the setup.

ID	Requirement	Traceability
T.1	Operational turning angle of $\phi = 0^\circ$ to $\phi = 360^\circ$	Chapter 3 introduction
T.2	Antenna gain $> 7 \text{ dBi}$	Section 2.2
T.3	Matching linear polarization	Section 2.1.2

Table 3.2: Table of technical requirements.

4 System Design

The full system includes a VNA, a turntable, two directional antennas and a computer. This chapter describes the interfaces between the individual parts and their functionalities. In order to get an overview of the full system consider figure 4.1.

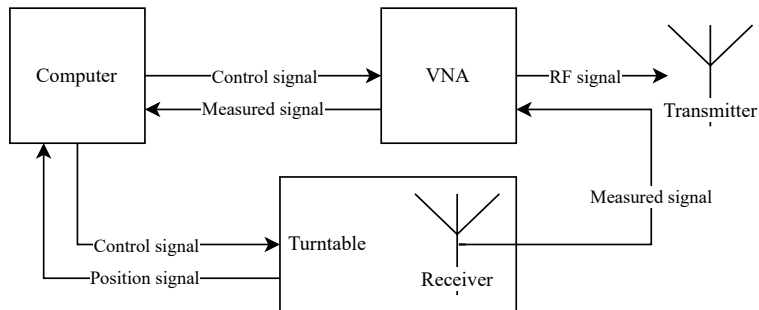


Figure 4.1: Overview of system design.

The system is composed of three integrated modules and two directional antennas. The first antenna is a transmitter antenna and the second antenna is a receiver antenna meant to rotate and measure gainm in different directions. These different directions are determined by the turning of the turntable on which the receiver antenna is mounted. Both the transmitter antenna and receiver antenna are connected to a VNA, but for the transmitter antenna, the functionality of the VNA used is the RF generator. For the receiver antenna, the received signal measured by the VNA is then further sent to the computer for data analysis. The computer controls the turntable and the VNA. This includes defining settings before the analysis and taking decisions based on the returned data; the position of the turntable and the measured antenna signal from the VNA.

4.1 Antenna Design

The most important characteristics of the antenna chosen for the design is that it is directional. The antenna must be directional in order to detect the direction of

transmission. The receiver and transmitter antenna must have the same polarization to ensure that this does not introduce loss in the system. The receiver antenna and the transmitter antenna are chosen to be the same type of antenna with the exact same shape for convenience. This means that all antenna parameters are the same.

The chosen antenna is a homemade, pyramidal horn antenna. It has a rectangle cross-section, straight curvature of the side walls and therefore a linear polarization. The size of the antenna is 10 cm by 7.65 cm giving an aperture area of 0.00765 m^2 . The remaining measurements can be seen on figure 4.2 on the right and a picture of the antenna on its mount on the left.

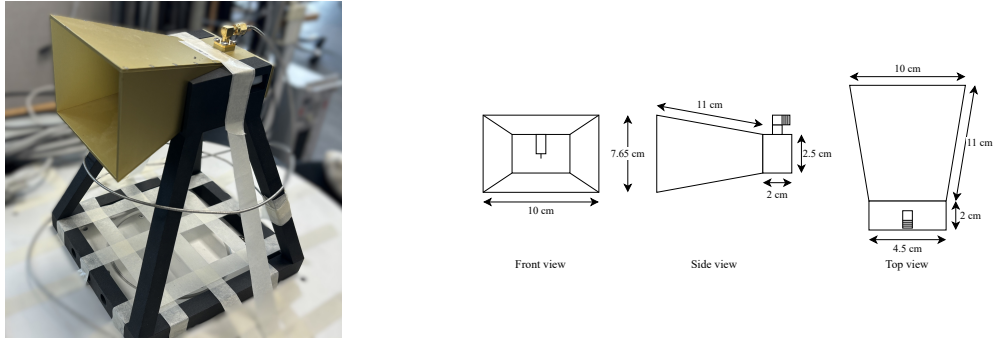


Figure 4.2: Horn antenna. Picture and diagram with measurements of horn antenna (not to scale).

In section 2.1.4 the effective aperture of an antenna is given in equation 2.12. Rewriting this equation to isolate the gain of the receiver antenna in dB gives

$$G_{r,dBi} = 10 \log_{10} \left(\frac{4\pi}{\lambda^2} A_r \right) \quad [\text{dB}] \quad (4.1)$$

The frequencies used for testing the system, 4.75 GHz and 5.65 GHz, have been chosen from the test results of S-parameter test in section B.1. The maximum theoretical gains at 4.75 GHz and 5.65 GHz, in the case of the maximum aperture efficiency of 1, are

$$G_{r,dBi,4.75} = 10 \log_{10} \left(\frac{4\pi}{\left(\frac{300E6}{4.75E9} \right)^2} 0.00765 \right) = 13.82 \quad [\text{dB}] \quad (4.2)$$

$$G_{r,dBi,5.65} = 10 \log_{10} \left(\frac{4\pi}{\left(\frac{300E6}{5.65E9} \right)^2} 0.00765 \right) = 15.33 \quad [\text{dB}] \quad (4.3)$$

The antenna has been tested as seen in section B.1 and B.2 to find the return loss S_{11} and the radiation pattern. The horn antenna has a S_{11} magnitude of -15.71 dB at 4.75 GHz and -19.56 dB at 5.65 GHz. The radiation pattern in the elevation and azimuth planes can be seen in figure B.2 and figure B.3. The horn antenna has 3 dB-bandwidths at 22.5° for $f = 4.75 \text{ GHz}$ and at 19° for $f = 5.65 \text{ GHz}$.

4.2 Choice of Turntable

The turntable must be able to be remotely controlled and precise, so that the angular position of the antenna can be determined confidently. The turntable must be able to turn to a remotely specified angle at each turn.

The *Head Acoustics, HRT I* turntable was available and fulfills the requirements. It has the ability to turn 360° with angle steps of 0.1° . It can be manually controlled and remotely controlled with software tools. It is able to turn at a maximum speed of 2 rpm by a step motor [9].

4.3 Choice of Vector Network Analyzer

The VNA must have a minimum of two ports, one for input and one for output, be able to be calibrated to normalize the transmission lines to the antennas and must be able to be remotely controlled. Moreover, it must cover the frequency range of the horn antennas. The *Rohde & Schwarz ZVB8* covers the range from 300 kHz to 8 GHz with 1 Hz resolution. It can have a measurement time of < 4.5 ms with simultaneous data transfer, which allows for fast execution of measurements. The internal noise level is frequency dependent and maximum < -70 dBm [17, p. 14].

4.4 Design of Software Control Program

Using a computer for the control of every aspect of the system allows for the devices to be programmed to operate concurrently. Both the VNA and the turntable are able to be controlled in *Python*. The control of the turntable is implemented as advised by the manual (see [10]) with the supplied software *RC-HRT I*. In order to control the turntable, the *RC-HRT I* software is interfaced via the *Python* module *pywin32*, which provides access to the Windows APIs [13]. *Rohde & Schwarz* have published a *Python* module for control of the VNA. The *Rohde & Schwarz* module adds an API for the remote control of the VNA, which is communicated with over TCP using SCPI-commands (*Standard Commands for Programmable Instruments*). Finally, thread parallelism is achieved with the module *threading*, which is what allows for the design of the control flow to work more efficiently by creating a thread for each device.

4.4.1 Communication Interfaces

The communication interfaces of the program is limited by the choice of the VNA and the turntable. The *HEAD Acoustics, HRT I* turntable that has been chosen can be controlled by serial communication using the RS485-standard [9]. However, it can also be controlled by its accompanying Windows driver and software control

program that accesses the Windows APIs. This requires the Windows registry to be updated with the UUID found in the control interface manual. With the Windows APIs accessible, the turntable can be controlled with predefined methods defined in the operating manual [11].

The *Rohde & Schwarz ZVB8 VNA* has a LAN type interface for control and data transfer [17, p. 5.3]. LAN allows for mutual communication between devices. LAN covers both the physical layer in the form of cabling and network cards, the latter which also contains part of the link layer in the form of logic decisions, and the link layer which includes the link protocol [5, p. 153]. In order to communicate across a LAN the computers must be connected to the same network and know each other's addresses [5, p. 174-175]. TCP ensures a connection between the two applications running on the computer and the VNA by a port number. Moreover, the TCP header includes an acknowledgement number which the applications use to acknowledge to each other, that the previous message was correctly received [5, p. 313]. The content of the TCP packets is SCPI commands and device-specific commands that follow the SCPI-standard [17, p. 5.4].

4.4.2 Concurrency

Because communication with the turntable and the turning process and communication with the VNA are both I/O bound tasks, there is a risk of wait time. Therefore, in order to achieve concurrent communication and data processing, the wait time is exploited by use of the Python module *threading*. *Threading* uses a single processor and pre-emptive multitasking to achieve concurrency [2]. This means that at any time if one thread is not using CPU computation the processor can switch to another thread and continue computation here. The processor also saves the current state of each thread so that it can return to the exact same place. This also means that reading and writing to global variables must be protected, because the processor can switch in the middle of a read/write statement. Likewise, if a thread needs to wait for another thread to execute a specific task, it is necessary that the user defines a wait flag, which synchronises the wait between relevant threads [2]. The *threading* module implements no option to set thread priorities or make scheduling principles [7].

5 Implementation

In this chapter the implementation of the software to control the turntable and the VNA is described based on the design principles laid out in Chapter 4. The background for the implementation is to fulfill the requirements set out in Chapter 3. In the project a Windows computer is used to interface to the turntable and VNA, and the software implementation is influenced by this choice.

The VNA and the turntable are controlled in *Python*. The source code is configured up to have a module for each device and a main control program. In the main control program the concurrency is implemented. The software is programmed with an object-oriented approach. Figure 5.1 shows how variables and methods are implemented in the VNA and turntable class, and how variables and functions are implemented in the main module.

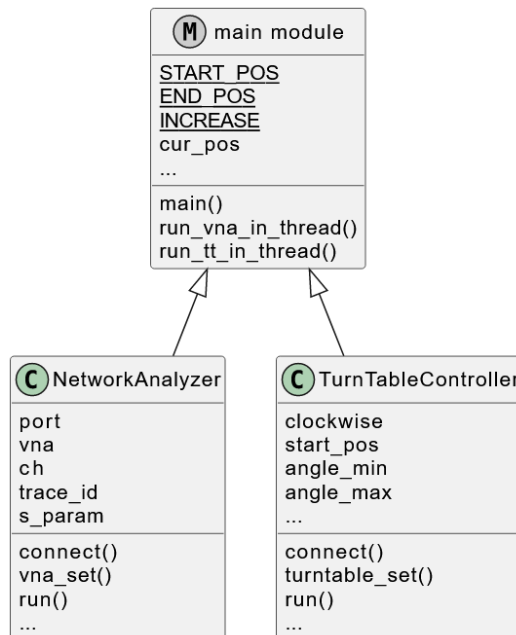


Figure 5.1: Diagram of VNA class, turntable class and main module implementation.

5.1 Turntable Control

As previously mentioned in Section 4.4.1 the turntable is controlled in *Python* with the *Pywin32* module that gives simple access to the Windows APIs. The turntable comes with a interface documentation document (see [11]) that elaborates on the functions that the turntable will accept. These are implemented in the control program.

First, a TurnTableController class is defined. The initialisation of the class will call the `__init__` method that creates the instance variables and tries to connect to the turntable. The connection is checked with a `if/elif/else` statement. If the connection is not possible, the error handler is set to exit the program. Else, if the connection is established the settings for the turntable will be set. The final `else` statement is used to catch any other state, which is treated as an error and the program is exited.

The turntable has multiple settings that need to be specified in order to ensure correct operation. These settings are set in the method `turntable_set` defined in the turntable class in the turntable module, see code in 5.1. The rpm and the acceleration function are predefined from the manufacturer and can be between 0 and 2 rpm and with four different levels of steepness in acceleration to full speed. Moreover, the turntable can either turn in a bipolar or unipolar direction. The desired unipolar direction is set, however, if this setting can not be made, the `angle_max` is updated from 360, the unipolar maximum, to 180, the bipolar maximum value. Lastly, the current position `cur_pos` is read and compared to the start position `start_pos` in a while loop, and the turntable is instructed to turn to the start position in the opposite direction of its normal turning direction.

```
1 def __init__(self, instance: str, ttc, clockwise: bool = False,
2     start_pos: float = 0.0, angle_min: float = ANGLE_MIN, angle_max:
3         float = ANGLE_MAX) -> None:
4     """ Initialize instance variables, connect and set settings."""
5     self.instance = instance
6     self.ttc = ttc
7     self.clockwise = clockwise
8     self.start_pos = start_pos
9     self.angle_min = angle_min
10    self.angle_max = angle_max
11    if self.ttc.Count == 0:
12        logger.error("No turntable is connected.")
13        exit()
14    elif self.connect() == EConnectionState.ecsConnectedOn.value:
15        self.turntable_set(rpm=2, func=EAccelerationFunction.afImpulse
16        , start_pos=self.start_pos)
17    else:
18        logger.error("Unknown error in startup sequence.")
19        exit()
```

```

18 def turntable_set(self, rpm: int, func: EAccelerationFunction, start_pos:
19     float) -> None:
20     """ Establish basic settings: rpm, acceleration function and start
21     position. """
22     cur_pos: int = round(self.position)
23     try:
24         self.tt.Velocity = rpm
25         self.tt.AccelerationFunction = func.value
26     except Exception as e:
27         logger.error(f"Unable to set settings for turntable {self.
28 instance}, exiting with error code {e}.")
29         exit()
30     if self.tt.DisplayPolarity == EPolarity.epolBipolar.value:
31         try:
32             self.tt.DisplayPolarity = EPolarity.epolUnipolar.value
33         except Exception:
34             self.angle_max = 180.0
35             logger.error(f"Unable to set polarity to unipolar for
36 turntable {self.instance}.")
37     while cur_pos != round(start_pos):
38         logger.info(f"Current position is {cur_pos} not start position
39 {round(start_pos)}. Moving {self.instance} to start position.")
40         if self.clockwise:
41             self.go_to_CCW(start_pos)
42         else:
43             self.go_to_CW(start_pos)
44         cur_pos = round(self.position)
45 logger.info(f"Settings are velocity: {round(self.tt.Velocity)},
46 function: {EAccelerationFunction(self.tt.AccelerationFunction)}")
47 logger.info(f"Current position for {self.instance} is {cur_pos}.")

```

Listing 5.1: Method to establish settings for turntable and reach start position.

The run method, see code 5.1, of the turntable takes the value of the increment inc as input argument and accesses the current position cur_pos and the value of the turning direction clockwise to determine and turn either in a clockwise or counter-clockwise direction. Finally the position is checked against the maximum and minimum angle values which are defined in the beginning of the module to be ANGLE_MIN = 0.0 and ANGLE_MAX = 360.0.

The step_CW method is equal to the step_CCW method except for the turning direction. First, the size of the step is set before the step is made, according to the definition in the turntable documentation. For the go_to_CW method, the interface method to be called is GoToCW which accepts the position in degrees as a floating point number as input. Both methods include the option to force the program to execute no other tasks while the turntable is turning which is done by setting the wait flag which will call the wait_while_driving method. This method calls time.sleep() which effectively utilises the active processor fully. The wait_while_driving method also includes a wait time check that will break

the wait while loop after the user defined timeout and allow the code to continue executing.

```

1 def run(self, inc: float) -> None:
2     """ Run the turntable. Changes the current position with [inc]
3     degrees. """
4     cur_pos: float = self.position
5     if self.clockwise:
6         self.step_CW(inc)
7     else:
8         self.step_CCW(inc)
9     if (self.angle_min > cur_pos > self.angle_max):
10        logger.error(f"Current position is illegal. Resetting: {self.instance}")
11        self.reset(self.instance, self.clockwise)
12
13 def step_CW(self, degrees, wait: bool = False) -> None:
14     """ Step [degrees] in clockwise direction. """
15     self.tt.StepSize = float(degrees)
16     self.tt.StepCW()
17     if wait:
18         self.wait_while_driving()
19
20 def go_to_CW(self, degrees: float, wait: bool = False) -> None:
21     """ Go to [degrees] while moving in clockwise direction. """
22     self.tt.GotoCW(float(degrees))
23     if wait:
24         self.wait_while_driving()
25
26 def wait_while_driving(self) -> None:
27     """ Ensures that the program waits for the turntable to reach
28     position before execution further code. """
29     seconds_waited = 0.0
30     while self.tt.IsMoving:
31         time.sleep(0.5)
32         seconds_waited += 0.5
33         if seconds_waited > 120:
34             logger.warning('Timeout while waiting for stop.')
35             break

```

Listing 5.2: Methods for turning the turntable to the wanted position.

The `reset` method, see code 5.1, used in the `run` method for position check will first call the `stop` method. This method will force stop the turntable by calling `MoveAbort()`. The `reset` method then rotates to the start position `start_pos` based on the setting of the `clockwise` boolean variable.

```

1 def stop(self) -> None:
2     """ Stop turning. """
3     if self.tt.IsMoving:
4         self.tt.MoveAbort()

```

```

5     logger.warning(f"Turntable was moving while connection was
6     stopped for {self.instance}.")
7     logger.info(f"Turntable {self.instance} is stopped.")
8
9 def reset(self) -> None:
10    """ Reset Turntable to start position. """
11    self.stop()
12    if self.clockwise:
13        self.go_to_CCW(self.start_pos)
14    else:
15        self.go_to_CW(self.start_pos)

```

Listing 5.3: Method for resetting the turntable to start position.

The turntable class includes a single attribute, which is the position of the turntable. The position is established as an attribute by using the `@property` decorator on the method returning the position variable. Setting the position as an attribute without a `setter` decorator ensures that the position variable becomes read-only.

5.2 VNA Control

The automation of the measurements with the VNA are made with the *Rohde & Schwarz* instrument library, that provides an easy interface instead of implementing the SCPI commands. Firstly, the connection with the VNA must be established. The IP address of the VNA has been manually set in the settings on the VNA and the assigned port has been extracted from the computer system.

The VNA control is implemented as a class object. In the `__init__` method of the class, see code 5.2, the connection is established to the VNA over TCP. Further, relevant settings are provided as class variables. This is for example the frequency on which the measurements must be made. This is provided as a floating point number when the VNA class is instantiated. The number of measurements, also called channel points, is also set in the `__init__` method to 1, since only one measurement needs to be made at one frequency. If the measurements should've been made over a frequency range, the `start_frequency_Hz` and `stop_frequency_Hz` could be modified accordingly and the number of measurements to be made in the range can be set with the `points` variable.

The `connect` method, see code 5.2, implements an exception handler in case the `open_tcp` method returns an error and exits the program, because it is not recommended to execute further without this connection. If the connection is successfully established a single channel with the identifier `ch=1` is created.

The specific S-parameter to be measured is also set when the class is instantiated. The value is used in the `vna_set` method that establishes the trace settings, such as which S-parameter to measure and the format of the measurements, which

is magnitude in dB.

```

1 def __init__(self, trace_id: str, s_param: str, freq: float,
2 ip_address = '172.0.0.1', port: int = 5025, channel = 1) -> None:
3     """ Initialize instance variables and connect.
4     Instrument Type: ZVB8 with 2 Ports
5     Part Number: 1145.1010k08
6     Serial Number: 100113
7     Device ID: 1145.1010K08-100113-DD
8     IEC Bus Address: 20
9     IP Addresses: IP Address 172.0.0.1 (localhost) Subnet Mask:
10    255.0.0.0 """
11    self.port: int = port
12    out: tuple = self.connect(ip_address, port, channel)
13    self.vna: Vna = out[0]
14    self.ch: Channel = out[1]
15    self.trace_id = trace_id
16    self.s_param = s_param
17    self.ch.start_frequency_Hz = freq, 'GHz'
18    self.ch.stop_frequency_Hz = freq, 'GHz'
19    self.ch.points = 1
20
21 def connect(self, ip_address: str, port: int, ch: int) -> tuple:
22     """ Try to connect to VNA with TCP. """
23     try:
24         sock = Vna()
25         sock.open_tcp(ip_address, port)
26     except Exception as e:
27         logger.error(f'Cannot connect to VNA because {e}.')
28         exit()
29     else:
30         logger.info(f'Connection established to VNA. Creating channel {ch}.')
31         channel = sock.channel(ch)
32     return sock, channel
33
34 def vna_set(self) -> None:
35     """ Establish trace for VNA. """
36     self.vna.create_trace(self.trace_id, 1, self.s_param)
37     self.vna.trace(self.trace_id).format = TraceFormat.magnitude_dB

```

Listing 5.4: Method for initialisation of VNA settings including creating VNA trace.

The run method, see code 5.2, returns the data measured formatted as a tuple with frequency at index 0 and power at index 1. The run method calls the trace method from the Vna class from the *Rohde & Schwarz* instrument library to retrieve the trace ID and calls the measure_formatted_data method on the trace variable.

```

1 def run(self) -> tuple:
2     """Measure S-Parameters for [trace_id]."""
3     x, y = self.vna.trace(self.trace_id).measure_formatted_data()

```

```
4     return x, y
```

Listing 5.5: Method for getting measurements from VNA.

The VNA can be completely reset by calling the `reset` method from the *Rohde & Schwarz* instrument library, however, this will also remove the calibration of the VNA that is performed to normalize the transmission line. The calibration data can be saved as a file and reopened for continuous use of the same calibration data. The calibration must therefore be performed manually before the execution of the setup, otherwise the data can be faulty.

5.3 Main Control Flow

The start and end positions and the angle increase are initialised as constants, see code 5.3. The current position `cur_pos` must be read both by the VNA thread and the turntable thread, and must be set by the turntable, therefore this variable is defined globally together with a lock `lock_cur_pos`, so that only one thread will access the variable at a time. Likewise with the variable for maximum position `max_pos` which also has its own event handler `max_pos_event_handler`, so that the turntable thread will wait for the VNA thread to find the maximum position before reading the variable and turning to that position.

```
1 START_POS = 10.0
2 END_POS = 150.0
3 INCREASE = 20.0
4
5 lock_cur_pos = Lock()
6 cur_pos: int = None
7
8 max_pos_event_handler = Event()
9 lock_max_pos = Lock()
10 max_pos: int = None
```

Listing 5.6: Global constants and variables.

The turntable is interfaced with the windows API made available with the *Pywin32* module. The code in line 2-3 in 5.3 in the `run_tt_in_thread` function is the initialisation of this interface. Then, the global variables are accessed via *Python's* `global` keyword. The current position is read from the `turntable.position` property defined in the *turntable* module. The while loop turns the turntable from the `START_POS` to the `END_POS` in increments of `INCREASE`. In the while loop, the turntable sets its own event handler `turntable_event_handler` to true to indicate to the VNA thread that it can now run, and then the turntable thread waits for the VNA thread. Hereafter the turntable turns and updates the current position `cur_pos`. Once the end position `END_POS` is reached, the while loop is exited and this is indicated to the VNA thread with the `end` event handler. Lastly, the

turntable thread turns to the maximum position `max_pos` when the VNA thread has indicated, that this variable has been set.

```

1 def run_tt_in_thread(ttc: CDispatch, turntable_event_handler: Event,
2 vna_event_handler: Event, end: Event, ttc_id) -> None:
3     CoInitialize()
4     ttc = Dispatch(CoGetInterfaceAndReleaseStream(ttc_id, IID_IDispatch))
5     turntable = TurnTableController(instance="hrt i (64980128)", ttc=ttc,
6         clockwise=True, start_pos=START_POS)
7
8     global cur_pos
9     global max_pos
10    count: int = 1
11
12    with lock_cur_pos:
13        cur_pos = round(turntable.position)
14
15    while START_POS <= cur_pos < END_POS:
16        turntable_event_handler.set()
17        turntable_event_handler.clear()
18        vna_event_handler.wait()
19        turntable.run(INCREASE)
20        with lock_cur_pos:
21            cur_pos = round(turntable.position)
22            logging.info(f"Current position for {turntable.instance} is
23 {cur_pos}.")
24            count += 1
25        turntable_event_handler.set()
26        turntable_event_handler.clear()
27        end.set()
28
29    max_pos_event_handler.wait()
30    with lock_max_pos:
31        if turntable.clockwise:
32            turntable.go_to_CW(max_pos)
33        else:
34            turntable.go_to_CCW(max_pos)
35
36    logging.info(f'Turntable thread is closed. {count} positions
37 measured.')

```

Listing 5.7: Thread function for running VNA.

The VNA thread `run_vna_in_thread`, see code 5.3, first accesses the global variables `cur_pos` and `max_pos`. Then two lists for measurement position `data_pos` and measured power `data_pow` are defined. The while loop for the VNA runs as long as the turntable thread has not set the `end` event handler to true, indicating that turning has finished. The while loop begins with waiting for the turntable to indicate it has finished turning with the `turntable_event_handler`. The power measurement is made with the execution of the code in line 10 in the VNA thread.

The two lists containing the measurement data are updated by first calling the current position lock `lock_cur_pos` before appending to the lists. When the turntable thread has indicated that turning is finished, the VNA thread immediately calculates the maximum position and updates the global `max_pos` variable.

```

1 def run_vna_in_thread(vna: NetworkAnalyzer, turntable_event_handler: Event, vna_event_handler: Event, end: Event) -> None:
2     global cur_pos
3     global max_pos
4     data_pos: list = []
5     data_pow: list = []
6     count: int = 0
7
8     while not end.is_set(): # run only when end == false
9         turntable_event_handler.wait()
10        _, pow = vna.run()
11        vna_event_handler.set()
12        vna_event_handler.clear()
13        logging.info(f'Power measurement is {pow}.')
14        with lock_cur_pos:
15            data_pos.append(cur_pos)
16            data_pow.append(pow)
17            count += 1
18
19        max_gain: float = max(data_pow)
20        with lock_max_pos:
21            max_pos = data_pos[data_pow.index(max_gain)]
22            logging.info(f'Max gain measured is {max_gain} at position {max_pos} .')
23        max_pos_event_handler.set()
24
25    logging.info(f'VNA thread is closed. {count} measurements made.')

```

Listing 5.8: Thread function for running VNA.

The main function, see code 5.3, has to create the setup for controlling the turntable with the Windows API in a thread, the VNA instance and trace settings, the two threads, event handlers, start the threads and ensure that both threads close correctly when finished by using the `join()` function on each thread.

```

1 def main():
2     logging.basicConfig(filename=f'./tests/test-{time.strftime("%Y%m%d-%H%M")}-log.txt', filemode='a', format='%(asctime)s:%(name)s: %(message)s', level=logging.INFO, datefmt='%Y-%m-%d %H:%M:%S')
3
4     CoInitialize()
5     ttc = Dispatch("TurnTableControlLib.TurnTableControl")
6     ttc_id = CoMarshalInterThreadInterfaceInStream(IID_IDispatch, ttc)
7
8     vna = NetworkAnalyzer(trace_id='trc1', s_param='s21', freq=5.65)
9     vna.vna_set()

```

```

10    logging.info(f'VNA with trace id {vna.trace_id} is created.')
11    Measuring {vna.s_param}.')
12
13    turntable_event_handler = Event()
14    vna_event_handler_handler = Event()
15    end = Event()
16
17    turntable_thread = Thread(target=run_tt_in_thread, kwargs={'ttc_id':
18        ttc_id, 'ttc': ttc, 'turntable_event_handler':
19        turntable_event_handler, 'vna_event_handler':
20        vna_event_handler_handler, 'end': end})
21    turntable_event_handler.clear()
22
23    vna_thread = Thread(target=run_vna_in_thread, kwargs={'vna': vna,
24        'turntable_event_handler': turntable_event_handler,
25        'vna_event_handler': vna_event_handler_handler, 'end': end})
26
27    turntable_thread.start()
28    vna_thread.start()
29
30    turntable_thread.join()
31    vna_thread.join()

```

Listing 5.9: Main function.

Calling the `main` function ensures that the entire setup, meaning the turning of the turntable and the measuring of magnitude of the received signal by the VNA, runs automatically before saving the data logs to a text file.

6 Measurement Results

This chapter includes test descriptions and results to validate the design against the requirements. First, the horn antennas are tested to find the gain and S_{11} -parameter. The descriptions and results of those tests can be found in appendix B.1 and B.2. Finally, the full test of the beam steering and gain measuring is tested with the transmitter fixed at a known location in the test area. The aim of this test is to determine the full functionality of the developed product. The test should show that the receiver antenna on the turntable is able to scan the test area and measure the received power at fixed angles, before selecting the location with the maximum received power and focusing its beam on that location. The test also contains test of intruder detection. In these scenarios the line-of-sight between the transmitter and receiver antennas is broken by an object. Figure 6.1 shows a simple diagram of the test setup from a horizontal view.

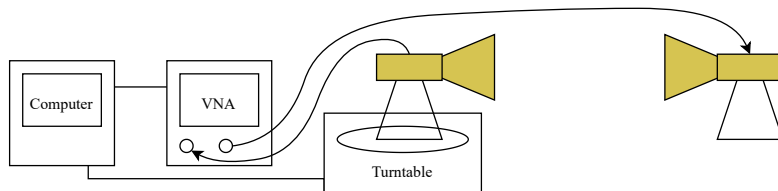


Figure 6.1: Setup for test of functionality of beam steering device.

6.1 Equipment

To perform the test, the following equipment is needed:

- *HEAD Acoustics Remote-operated Turntable, model HRT I 6498* with 24 V DC 60 W power supply
- D-sub 9-pin to USB-A cable to connect turntable to PC
- PC with one USB-A port and one LAN port
- *Rohde & Schwarz ZVB8 Vector Network Analyzer*

- Network cable (8-pin RJ-45 connector) to connect VNA to PC
- Two identical horn antennas with dimensions as seen on figure 4.2 in section 4.1
- Two 50Ω antenna cables
- Two identical horn antennas as DUTs.

Moreover, the test must be performed in a controlled environment in order to ensure that the turntable and VNA can function optimally. The temperature must not be below 5°C or above 40°C with a relative humidity in the range 20% - 80% [9][17].

6.2 Procedure

The following steps outline how to perform the test:

1. Power ZVB8 and HRT I.
2. Calibrate ZVB8 with calibration unit.
3. Connect Windows PC to ZVB8 and HRT I.
4. Connect transmitter antenna to port 2 on ZVB8 with antenna cable. Set channel power level to 10 dBm.
5. Connect receiver antenna to port 1 on ZVB8 with antenna cable.
6. Setup transmitter antenna to point in a direction defined by the setup configuration.
7. Mount the receiver antenna on HRT I.
8. Load *Python* code on Windows PC and run control program.

Repeat the test procedure for different setups; antennas pointing straight to each other with and without intruder person, with the antennas in either corner of a room with and without intruder table, and with the transmitter perpendicular to the receiver antenna.

6.3 Test Results

The tables in the following sections include condensed versions of the logs printed with every test of the full setup. The logs can be found through the link in appendix A.

6.3.1 Straight Setup

This test scenario is made with the antennas pointing directly towards each other without intruder. The distance between the antennas is $d = 5.4\text{ m}$. The start position is 10° , the end position is 150° and the increase is 20° . The following figure 6.2 shows the setup:

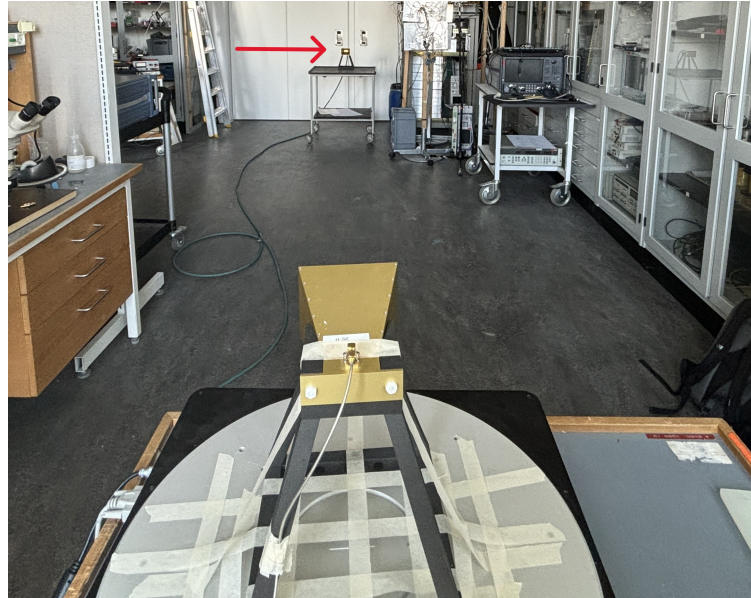


Figure 6.2: View from receiver antenna at position 50° towards transmitter antenna.

The test results can be found in table 6.1 and 6.2.

Frequency = 4.75 GHz			
Position (degrees)	Power Measurement (dB)		
	Test 1	Test 2	Test 3
10	-51.33	-51.15	-51.01
30	-46.82	-46.63	-46.52
50	-46.96	-46.77	-46.66
70	-49.07	-48.88	-48.78
90	-55.30	-55.18	-55.07
110	-70.33	-69.99	-69.81
130	-67.82	-67.30	-67.27
150	-66.85	-66.73	-66.58

Table 6.1: Table of power measurements at each position repeated three times at frequency $f = 4.75\text{ GHz}$. The maximum gain of each test is highlighted in red.

Frequency = 5.65 GHz			
Position (degrees)	Power Measurement (dB)		
	Test 1	Test 2	Test 3
10	-45.96	-46.04	-45.99
30	-34.88	-34.81	-34.76
50	-31.05	-30.99	-30.93
70	-34.61	-34.56	-34.51
90	-49.59	-49.54	-49.47
110	-64.89	-64.79	-64.67
130	-50.16	-50.15	-50.15
150	-58.68	-58.68	-58.79

Table 6.2: Table of power measurements at each position repeated three times at frequency $f = 5.65\text{ GHz}$. The maximum gain of each test is highlighted in red.

Comparing the results of the direct, straight line-of-sight without intruder between $f = 4.75\text{ GHz}$ and $f = 5.65\text{ GHz}$ it is seen that the maximum gain is not in the same direction but instead at 30° at $f = 4.75\text{ GHz}$ and at 50° at $f = 5.65\text{ GHz}$. Looking at the data for $f = 4.75\text{ GHz}$, it can be seen that the difference in magnitude from 30° to 50° is very small ($<0.14\text{ dB}$) where its larger ($>3.82\text{ dB}$) for $f = 5.65\text{ GHz}$ for the same angle step. This indicates that at $f = 5.65\text{ GHz}$ the beam of the horn antenna is narrower. The maximum gain is also larger at $f = 5.65\text{ GHz}$ at averagely 30.99 dB compared to the gain at $f = 4.75\text{ GHz}$ at averagely -46.66 dB .

6.3.2 Straight Setup With Intruder

The test scenario *straight with person intruder* is made with the antennas pointing directly towards each other. The distance between the antennas is $d = 5.4\text{ m}$ and the object, the person, is placed 2 m from the transmitter and 3.4 m from the receiver. The start position is 10° , the end position is 150° and the increase is 20° . The following figure 6.3 shows the setup:

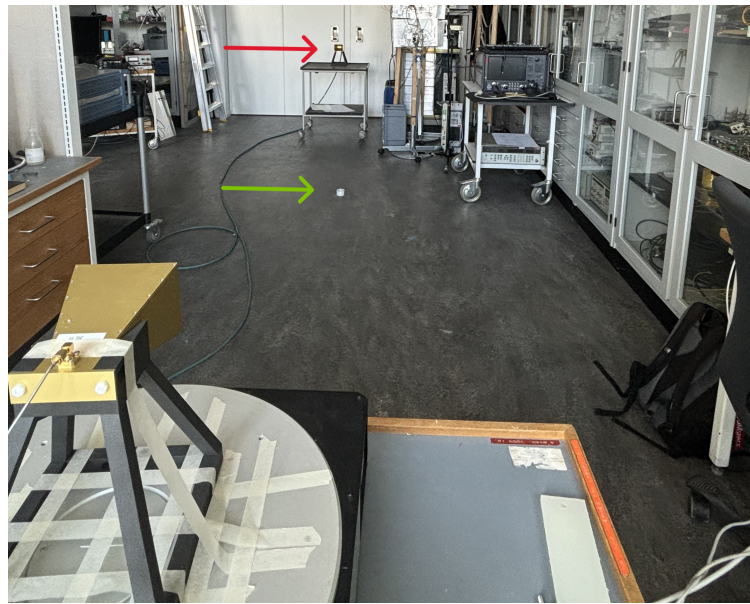


Figure 6.3: View from receiver antenna at position 50° towards transmitter antenna. The green arrow points towards the location where the person is.

The test results can be found in table 6.3 and 6.4.

Frequency = 4.75 GHz			
Position (degrees)	Power Measurement (dB)		
	Test 1	Test 2	Test 3
10	-53.88	-51.03	-53.15
30	-65.65	-62.04	-58.07
50	-60.18	-60.21	-63.31
70	-60.91	-61.45	-63.88
90	-68.03	-64.38	-67.73
110	-78.76	-67.41	-85.01
130	-68.04	-86.78	-72.53
150	-65.90	-66.63	-64.46

Table 6.3: Table of power measurements at each position repeated three times at frequency $f = 4.75\text{ GHz}$. The maximum gain of each test is highlighted in red.

Frequency = 5.65 GHz			
Position (degrees)	Power Measurement (dB)		
	Test 1	Test 2	Test 3
10	-48.58	-44.45	-44.61
30	-49.91	-55.05	-49.71
50	-43.50	-45.52	-39.29
70	-44.11	-45.39	-40.85
90	-54.07	-62.36	-50.56
110	-63.50	-74.10	-59.50
130	-52.11	-53.01	-52.56
150	-60.54	-57.75	-58.38

Table 6.4: Table of power measurements at each position repeated three times at frequency $f = 5.65\text{ GHz}$. The maximum gain of each test is highlighted in red.

The intruder changes the ability of the control program to correctly identify the direction of the transmitter antenna. At $f = 4.75\text{ GHz}$ the maximum gain is at 10° which is in the direction of the close wall on the right-hand side when facing the transmitter.

Further, the test data (seen in table 6.3) also show that the gain at 50° and 70° is averagely higher than at other angle steps, indicating that the receiver antenna still can detect the transmitter with a person intruder, but that the intruder does affect the received signal. At $f = 5.65\text{ GHz}$ the data is not consistent across all three tests. The receiver antenna receives the maximum gain in the same direction as the transmitter antenna in the line-of-sight test scenario.

When comparing to the same setup without intruder, where the maximum gain is also at 50° , it can be seen that the intruder does not dampen the signal to a level, where the reflection signal are larger than the direct, transmitted signal. Comparing the values, the maximum gain measured with an intruder is averagely $42.41\text{ dB} - 30.99\text{ dB} = 11.42\text{ dB}$ less than without intruder. In this scenario the frequency $f = 4.75\text{ GHz}$ can be a better frequency choice.

6.3.3 Corner-To-Corner Setup

This test is performed with the antennas pointing directly towards each other from a skew angle in each their own corner of the room. The distance between the antennas is not measured. The start position is 10° , the end position is 150° and the increase is 20° . The following figure 6.4 shows the setup:

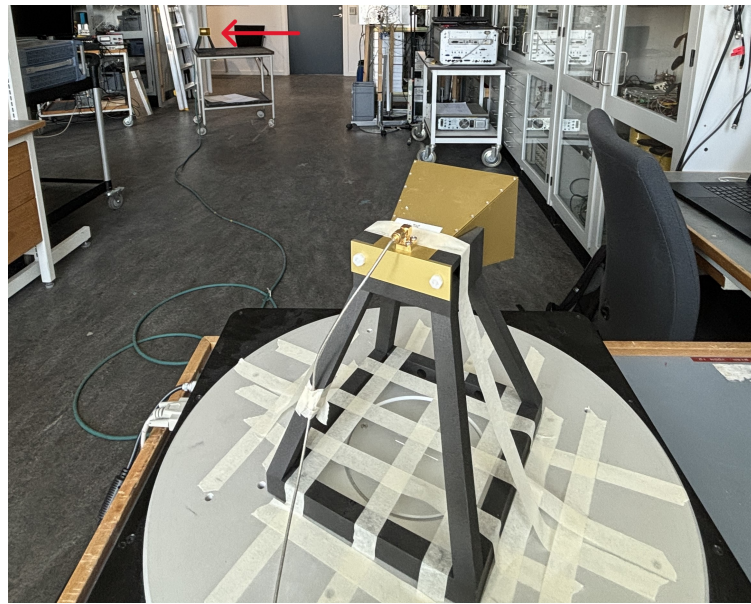


Figure 6.4: View from receiver antenna at position 10° towards transmitter antenna.

The test results can be found in table 6.5 and 6.6.

Frequency = 4.75 GHz			
Position (degrees)	Power Measurement (dB)		
	Test 1	Test 2	Test 3
10	-59.79	-59.20	-59.13
30	-52.45	-52.08	-52.00
50	-53.22	-52.94	-52.86
70	-48.34	-48.11	-48.06
90	-51.32	-51.09	-51.04
110	-70.33	-58.41	-58.33
130	-75.39	-75.27	-75.29
150	-62.40	-62.15	-62.07

Table 6.5: Table of power measurements at each position repeated three times at frequency $f = 4.75$ GHz. The maximum gain of each test is highlighted in red.

Frequency = 5.65 GHz			
Position (degrees)	Power Measurement (dB)		
	Test 1	Test 2	Test 3
10	-45.73	-45.41	-45.37
30	-43.94	-43.82	-43.79
50	-34.21	-34.01	-33.96
70	-32.29	-32.15	-32.10
90	-37.35	-37.27	-37.23
110	-51.65	-51.62	-51.63
130	-68.07	-68.20	-68.02
150	-56.72	-56.73	-56.66

Table 6.6: Table of power measurements at each position repeated three times at frequency $f = 5.65\text{ GHz}$. The maximum gain of each test is highlighted in red.

The test data with the corner-to-corner scenario shows the gain when the antennas are placed further apart in a corner-to-corner configuration with and without a table with a large, square electronic box as intruder. As seen on figure 6.4 the transmitter antenna is moved to the left, meaning that the turntable must turn further in order to face the receiver antenna towards the transmitter antenna. This reflects in the results in table 6.5 and 6.6 where both at $f = 4.75\text{ GHz}$ and $f = 5.65\text{ GHz}$ the maximum gain is at 70° . Similarly as with the straight line-of-sight setup (seen in figure 6.5) the maximum gain is larger at the higher frequency.

6.3.4 Corner-To-Corner Setup With Intruder

The test scenario *corner-to-corner with table intruder* is made with the transmitting antenna pointing in the direction of the receiver antenna, with the antennas each in an opposite corner. The distance between the antennas is not measured. The start position is 10° , the end position is 150° and the increase is 20° . The following figure 6.5 shows the setup:

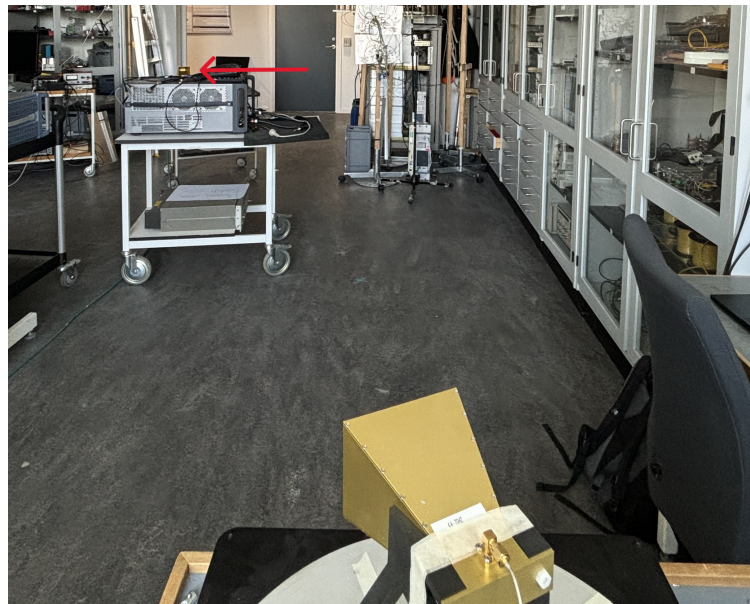


Figure 6.5: View from receiver antenna at position 70° towards transmitter antenna.

The test results can be found in table 6.7 and 6.8.

Frequency = 4.75 GHz			
Position (degrees)	Power Measurement (dB)		
	Test 1	Test 2	Test 3
10	-57.75	-57.52	-57.40
30	-59.87	-59.68	-59.57
50	-65.42	-65.22	-65.14
70	-62.53	-62.40	-62.26
90	-59.81	-59.60	-59.49
110	-64.94	-64.81	-64.74
130	-68.94	-68.80	-68.63
150	-62.11	-61.96	-61.85

Table 6.7: Table of power measurements at each position repeated three times at frequency $f = 4.75$ GHz. The maximum gain of each test is highlighted in red.

Frequency = 5.65 GHz			
Position (degrees)	Power Measurement (dB)		
	Test 1	Test 2	Test 3
10	-42.72	-42.68	-42.61
30	-47.23	-47.15	-47.10
50	-35.61	-35.55	-35.49
70	-35.83	-35.75	-35.69
90	-41.75	-41.68	-41.61
110	-54.32	-54.25	-54.20
130	-77.38	-76.43	-76.11
150	-57.60	-57.49	-57.27

Table 6.8: Table of power measurements at each position repeated three times at frequency $f = 5.65\text{GHz}$. The maximum gain of each test is highlighted in red.

The test is performed again with a table as an intruder. At $f = 4.75\text{GHz}$ the maximum gain is at position 10° which is not in the direction of the transmitting antenna but rather towards the right-hand wall when viewing from the receiver into the measurement space. This indicates that the receiver antenna receives reflections from the wall surface rather than directly from the transmitter. At $f = 5.65\text{GHz}$ this changes however, and the maximum gain is averagely 35.55 dB at position 50° .

The gain is approximately the same at position 70° as at position 50° with averagely difference of 0.21 dB , which is the direction of the transmitter antenna. This indicates that even with an intruder, the receiver is able to locate the transmitter when at the frequency $f = 5.65\text{GHz}$. Comparing with the test without intruder, it can be seen at 70° there is a significant difference in what is measured in both tests and a comparable result at 50° . This indicates that the table intruder dampens the signal at 70° exactly and that the intruder can be detected when comparing the two signals at 70° . In this scenario the frequency $f = 5.65\text{GHz}$ can be a better frequency choice.

6.3.5 Perpendicular Antennas

The test scenario is made with the transmitting antenna pointing perpendicular to the receiver antenna. The distance between the antennas is $d = 5.4\text{ m}$. The start position is 10° , the end position is 150° and the increase is 20° . The following figure 6.6 shows the setup:



Figure 6.6: View from receiver antenna at position 50° towards transmitter antenna.

The test results can be found in table 6.9 and 6.10.

Frequency = 4.75 GHz			
Position (degrees)	Power Measurement (dB)		
	Test 1	Test 2	Test 3
10	-74.27	-74.29	-74.33
30	-72.12	-72.13	-72.21
50	-77.03	-76.04	-75.61
70	-71.35	-71.17	-70.58
90	-69.45	-69.47	-69.71
110	-68.42	-68.28	-68.15
130	-79.83	-80.25	-79.30
150	-75.04	-75.25	-75.23

Table 6.9: Table of power measurements at each position repeated three times at frequency $f = 4.75 \text{ GHz}$. The maximum gain of each test is highlighted in red.

Frequency = 5.65 GHz			
Position (degrees)	Power Measurement (dB)		
	Test 1	Test 2	Test 3
10	-58.25	-58.25	-58.34
30	-55.13	-55.12	-54.97
50	-49.13	-49.11	-49.08
70	-52.44	-52.40	-52.43
90	-50.17	-50.10	-50.10
110	-49.77	-49.73	-49.81
130	-52.26	-52.20	-52.26
150	-58.72	-59.04	-58.64

Table 6.10: Table of power measurements at each position repeated three times at frequency $f = 5.65\text{ GHz}$. The maximum gain of each test is highlighted in red.

The transmitter antenna is placed perpendicular to the receiver facing the right-hand wall when looking from the receiver to the transmitter in a straight line. The setup can be seen in figure 6.6. At $f = 4.75\text{ GHz}$ the angle step with maximum gain is 110° which is not in the direction of the transmitter but instead in the opposite direction where the receiver antenna faces walls and tables with test equipment. This shows that the receiver antenna is unable to detect the transmitter at $f = 4.75\text{ GHz}$ if the transmitter is facing perpendicular to the the receiver antenna position.

At $f = 5.65\text{ GHz}$ the receiver antenna correctly identifies the transmitter to be at angle step 50° . This indicates that at $f = 5.65\text{ GHz}$ the gain of the transmitter antenna at the $\theta = 90^\circ$ angle in the azimuth plane is so large, that the receiver still detects the signal instead of reflections from objects in the measurement space.

6.4 Test Results Comparison

A further analysis of the test data can be made by comparing the measured gain at each position for all scenarios but excluding the perpendicular setup. The data is plotted in figure 6.7 for $f = 4.75\text{ GHz}$ and in figure 6.8 for $f = 5.65\text{ GHz}$. At $f = 4.75\text{ GHz}$ the graph shows that the intruder clearly dampens the received signal in both scenarios. The test data at this frequency is not consistent across test scenarios and positions.

The measured gain for test of the corner-to-corner with intruder increases in the position 70° to 90° where it decreases in the corner-to-corner without intruder test. This indicates that some signal is not blocked by the intruder at this position. The intruder in the straight test scenario dampens the measured gain from 30° to 110° . The decrease of the measured gain of the straight test with intruder is similar to the decreasing development of the measured gain without intruder as

the position increases from 30° to 110° .

The received signal present at 110° to 150° is not very consistent. This could indicate that there is unwanted signal disturbance or signal sources. The direction is far from the signal source, the transmitter antenna. In this direction reflections from vertical objects in the measurement space create reflections which can explain the increase in measured gain at 150° .

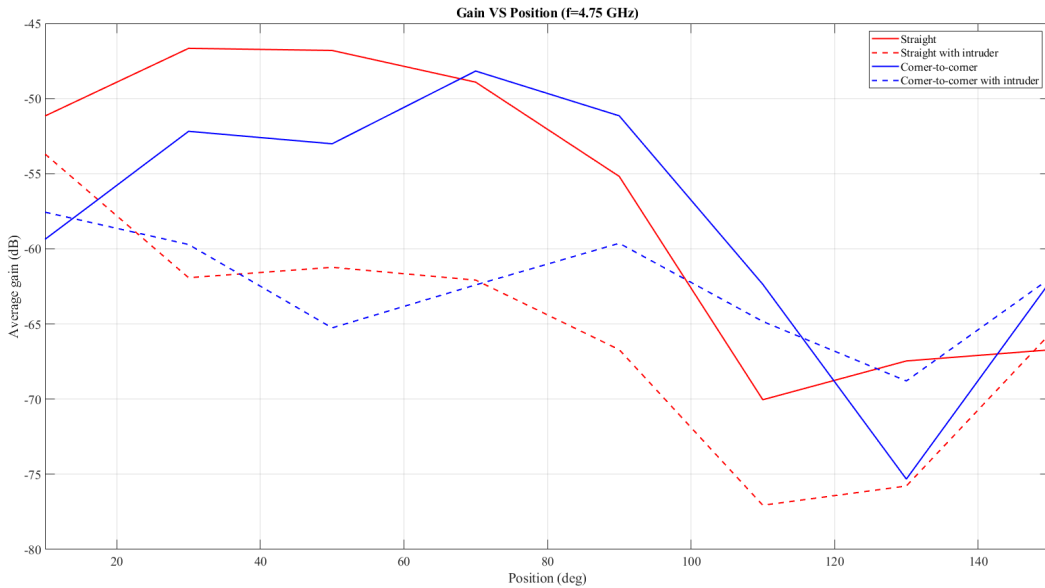


Figure 6.7: Measured gain at $f = 4.75$ GHz each position for the four scenarios straight or corner-to-corner and with or without intruder.

The tests performed at $f = 5.65$ GHz show a more clear trend when comparing each test scenario. The intruder clearly dampens the input throughout the entire position spectrum until the final position 150° , indicating that this position is in a direction too far away from the transmitter to be mainly influenced by the transmitted signal and is instead receiving a reflected signal. The measured gain in all four test scenarios is similar at this position.

The difference between the measurement with and without intruder is largest for the straight setup. The intruder was in the straight scenario a person, whereas in the corner-to-corner scenario the intruder was a table. This indicates that the size of the intruder affects the ratio of measured gains. Finally, the difference in the placement of the transmitter antenna can be most clearly seen without intruder, where the maximum gain is at 50° in the straight test scenario and at 70° in the corner-to-corner test.

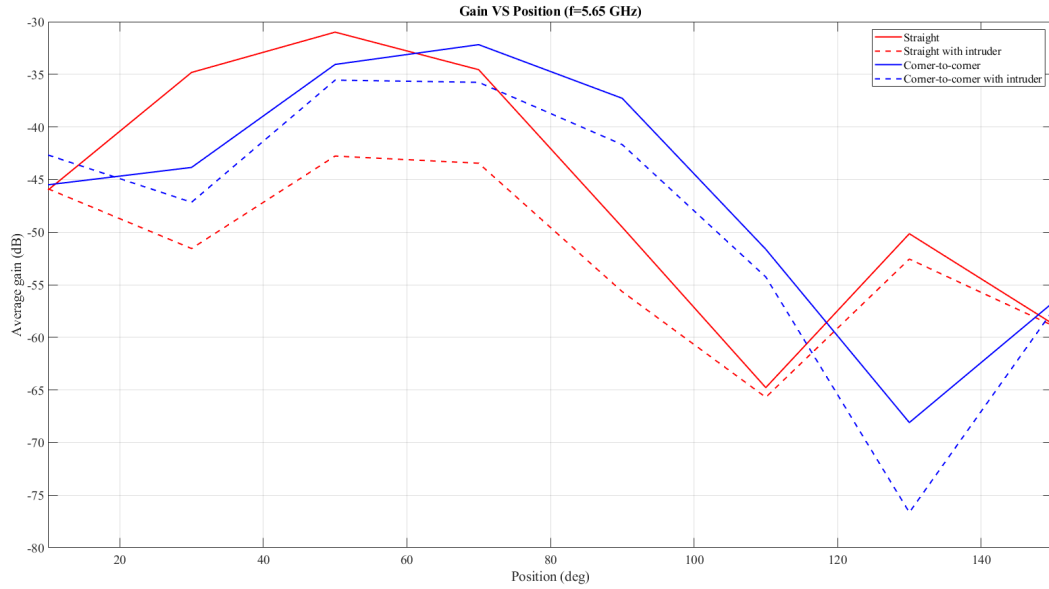


Figure 6.8: Measured gain at $f = 5.65\text{ GHz}$ each position for the four scenarios straight or corner-to-corner and with or without intruder.

The accept test show that at $f = 5.65\text{ GHz}$ more power is received which is because, as shown in test of radiation pattern B.2, that the horn antenna has a higher gain at this frequency than at the lower frequency tested.

While the turntable is turning the cable connected to the horn antenna will move with it. This will affect the phase of the signal. However, since the purpose of the test is to measure magnitude, this error is will not effect the test result. The test of the setup with a person as intruder is subject to measurement inaccuracies due to minimal movement.

7 Discussion

The aim of this project as set out in the introduction is to steer an antenna beam to detect a transmitter and focus the beam there, and also to detect an intrusion between the transmitter and the receiver. The turntable allows for mechanical beam steering in horizontal plane. This limits the ability to detect intruders to the horizontal plane, centered at the level of the antenna, meaning the setup for example would be unable to detect drones or small remote-controlled vehicles. The setup will not be able to detect intrusion above or below this level of the antenna, limiting the functionality of the setup. The control program with the electrically controlled mechanical turntable allows for the setup to be entirely automated. To have efficient intruder detection an automated setup must be a minimal requirement which the tests does show is possible.

The accept test was performed at the two frequencies 4.75 GHz and 5.65 GHz. There are clear differences between each frequency in all tests, showing that the choice of frequency affects the result. Other frequencies could have been chosen, as seen in the test of S_{11} in section B.1, that have a lower reflection coefficient than 4.75 GHz. At 5.65 GHz the tests show that even with an intruder between the transmitter and receiver, the receiver can locate the general direction of the transmitter and not only reflections in the measurement area. However, the gain in the direction of the transmitter is significantly reduced, therefore, when comparing the measured gain with and without intruder the setup could be expanded to use this comparison to alert of an intruder. The measured gain is also generally higher at 5.65 GHz than at 4.75 GHz at all angle positions. A more directive antenna could improve the setup by giving higher granularity of the position steps allowing for more accurate intruder location detection and by giving larger gain measurements for better differentiation at the angle steps. The latter, of which is also achieved with the horn antenna resonance frequency at 5.65 GHz rather than 4.75 GHz.

The test with the antennas perpendicular to each other shows that the layout of the test space greatly affects the measurements by giving different reflections at different positions and that with the setup of a transmitter antenna and receiver antenna, the result is best with the antennas facing each other. This dual-antenna

setup adds another requirement to the setup, which is that the antennas must have matching polarization and function at the same frequency. In this case, choosing two identical horn antennas is a solution.

The control program has been written in *Python* using the *threading* module in order to achieve concurrency. The I/O operations of the communication with the turntable and the VNA allow for some wait time to be exploited when using *threading*, but the control program does also contain computational statements, such as appending and comparing data variables and calculating the maximum gain position. These must be performed sequentially and therefore do not benefit from concurrency. Further, the control program is not implemented to run endlessly, and will stop after calculating the maximum gain position. To achieve intruder detection alertion, the program should run indefinitely and be able to show an alarm. In the case of sending an alarm, the concurrency with the *threading* module can be used further to make the control program be able to continue turning and measuring while reporting data or alerting a user of intrusion.

8 Conclusion

The turntable *HEAD Acoustics HRT I* is a mechanical turntable controlled that can turn 360° in the horizontal plane and it is controlled in a *Python* implemented control program, together with a *Rohde and Schwarz ZVB8* vector network analyzer. The choices of external devices ensures that the system requirements are met and the implementation, with the *Python threading* module, of the device control and communication with concurrency allows for efficient measuring. A number of possible antenna designs for a directive antenna can be used, however, two identical horn antennas where chosen because the chosen horn antenna type has a high directivity and matching polarization. The horn antennas are designed for 4.4GHz to 7GHz and have S_{11} -parameter of -19.56 dB and maximum gain of 12.99 dB at 5.65GHz and S_{11} -parameter of -15.71 dB and maximum gain of 11.41 dB at 4.75GHz. These two frequencies are used for test of full system.

The accept test shows that with a straight-line setup and with a corner-to-corner setup it is possible to see, in the comparisons with and without object blocking the line-of-sight, an intruder in the measurement area. The test also shows that the measurements at $f = 5.65\text{ GHz}$ all have a higher maximum gain and that the receiver antenna is generally able to detect the transmitter even with an intruder. The intruder dampens the received signal significantly, which is shown in the gain difference with and without intruder. Therefore, it can be concluded that the system can be used to detect an intruder when transmitting at both 4.75GHz and 5.65GHz when the transmitter faces the receiver.

Bibliography

- [1] GCM A/S. *Open vs. Closed Loop*. gearcentralen.dk/en/open-vs-closed-loop. Online; accessed 16-May-2024. u.a.
- [2] Jim Anderson. *Speed Up Your Python Program With Concurrency*. realpython.com/python-concurrency. Online; accessed 05-April-2024. u.a.
- [3] Peter Bevelacqua. *Bandwidth*. antenna-theory.com/basics/bandwidth.php. Online; accessed 04-May-2024. 2015.
- [4] Peter Bevelacqua. *The Dipole Antenna*. antenna-theory.com/antennas/dipole.php. Online; accessed 04-May-2024. 2015.
- [5] Libor Dostálek and Alena Kabelová. *Understanding TCP/IP*. First edition. Packt Publishing Limited, 2006.
- [6] Hans Ebert and Povl Raskmark. *Grundlæggende Maxwellsk Feltteori*. Fourth edition. Aalborg Universitet, 1998.
- [7] Python Software Foundation. *threading - Thread-based parallelism*. docs.python.org/3/library/threading.html. Online; accessed 23-May-2024. 2024.
- [8] Sujanth Narayan. K. G, Velavikneshwaran. V, and James A. Baskaradas. "Design of Electronically Steerable Direction Shifting Microstrip Antenna Array using Beam Steering Technique". In: *2021 IEEE Indian Conference on Antennas and Propagation (InCAP)*. 2021, pp. 60–63.
- [9] HEAD Acoustics GmbH. *Data Sheet HRT I*. cdn.head-acoustics.com/fileadmin/data/global/Datasheets/Data_Acquisition/HRT-I-Turntable-6498-Data-Sheet.pdf. Online; accessed 09-March-2024. 2023.
- [10] HEAD Acoustics GmbH. *HRT I Manual*. 2019.
- [11] HEAD Acoustics GmbH. *HRT I Turntable Control Interface Documentation*. 2018.
- [12] Isarsoft GmbH. *What is Physical Intrusion Detection?* isarsoft.com/knowledge-hub/intrusion-detection. Online; accessed 17-May-2024. 2024.
- [13] Mark Hammond. *Pywin32*. pypi.org/project/pywin32. Online; accessed 15-April-2024. u.a.

- [14] Andrea M. Mitofsky. *Direct Energy Conversion*. First edition. Trine University, 2018.
- [15] Electronics Notes. *Beamforming and Beamsteering Antennas*. [electronics-not es.com/articles/antennas-propagation/phased-array-antennas/beamf orming-beamsteering-antenna-basics.php](http://electronics-notes.com/articles/antennas-propagation/phased-array-antennas/beamforming-beamsteering-antenna-basics.php). Online; accessed 16-May-2024. u.a.
- [16] ITU Radiocommunication Sector. *Multipath Propagation And Parameterization Of Its Characteristics*. Tech. rep. International Telecommunication Union, 2021.
- [17] Rohde and Schwarz GmbH. *ZVB Vector Network Analyzer Specification*. [scdn .rohde-schwarz .com/ur/pws/dl_downloads/dl_common_library/dl_b rochures_and_datasheets/pdf_1/ZVB_dat_sw_en.pdf](http://scdn.rohde-schwarz.com/ur/pws/dl_downloads/dl_common_library/dl_b rochures_and_datasheets/pdf_1/ZVB_dat_sw_en.pdf). Online; accessed 05-April-2024. 2011.
- [18] Ming Shen. "Wireless Phy/Mac Fundamentals". Lecture notes; accessed 3-May-2024. 2014.
- [19] Chen Shun-Ping and Heinz Schmiedel. *RF Antenna Beam Forming*. First edition. Springer Cham, 2023.
- [20] Ankit Singh et al. "Beam steering in antenna". In: *2017 International Conference on Innovations in Information, Embedded and Communication Systems (ICIIECS)*. 2017, pp. 1–4.
- [21] Cadence PCB Solutions. *S-Parameters and the Reflection Coefficient*. [resources .pcb.cadence.com/blog/2023-s-parameters-and-the-reflection-coeff icient](http://resourcespcb.cadence.com/blog/2023-s-parameters-and-the-reflection-coeff icient). Online; accessed 3-May-2024. u.a.
- [22] Johann Tang. *The Choice Between Servo Motors and Stepper Motors*. [blog.orien talmotor.com/the-choice-between-servo-motors-and-stepper-motors](http://blog.orientalmotor.com/the-choice-between-servo-motors-and-stepper-motors). Online; accessed 16-May-2024. 2021.
- [23] John L. Volakis. *Antenna Engineering Handbook*. Fourth edition. McGraw-Hill Professional, 2007.

A Source Code Link

The repository containing the source code, test results and the report can be found at github.com/rikkeskov/p5-beam-steering.

B Test of Antenna Characteristics

B.1 Test of Horn Antenna S-Parameters

The aim of this test is to find S_{11} and the reflection coefficient of the receiving antenna. The measurement will be used to choose the resonance frequency for the acceptance test.

B.1.1 Equipment

To perform the test the following equipment is needed:

- Rohde & Schwarz ZNA Vector Network Analyzer (10 MHz-43.5 GHz)
- Rohde & Schwarz ZN-Z54 Calibration Unit (9 kHz-40 GHz)
- 50Ω antenna cable
- DUT - horn antenna

B.1.2 Procedure

The test is performed once. The following explains the procedure for the test:

1. Add power to VNA, connect antenna cable to VNA and Calibration unit.
2. Make calibration test by choosing *Cal* → *Quick Start Calibration* → *Apply* on the VNA.
3. Disconnect antenna cable and reconnect to DUT.
4. Set start and stop frequencies.
5. Ensure that VNA measures S_{11} -parameter by choosing *Meas* → S_{11} .

The antennas are identical horn antennas which are designed to work in the spectrum from 4 GHz to 7 GHz. The measurement is performed in the spectrum 3 GHz to 8 GHz in order to encapsulate the entire antenna frequency spectrum, with steps of 25 MHz.

B.1.3 Result

The following figure shows S_{11} as a function of frequency. The criterion considered for impedance matching is a reflection coefficient of -10 dB. In order to perform the measurements, the two resonance frequencies (4.75 GHz and 5.65 GHz) have been chosen.

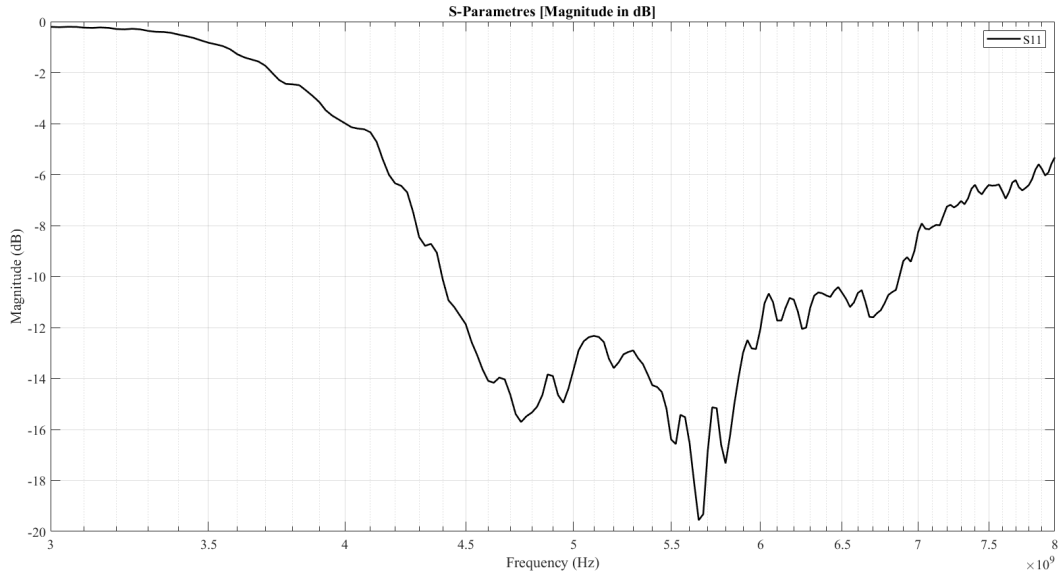


Figure B.1: Measured S_{11} -parameter from 3 GHz to 8 GHz.

It can be seen that the antenna has a maximum S_{11} magnitude of -19.56 dB at 5.65 GHz. This gives a reflection coefficient of $\Gamma = 10^{-19.56/20} = 0.11$. Almost 1 GHz away at 4.75 GHz the magnitude of S_{11} is -15.71 dB which equals a reflection coefficient of $\Gamma = 10^{-15.71/20} = 0.16$.

B.2 Test of Horn Antenna Radiation Pattern

The aim of this test is to know the directiveness of the antennas to obtain the 3 dB bandwidth of the antennas and determine the step angle needed in the turntable.

B.2.1 Equipment

The test is performed in the anechoic chamber at Aalborg University with the provided setup equipment at the site. This includes:

- Computer with relevant *MVG software*
- *MVG StarMIMO* in anechoic chamber

The MVG *StarMIMO* has a measurement bandwidth of 400 MHz to 6 GHz. As seen in the results in the test of S-parameters in subsection B.1 the maximum reflection coefficient magnitude is at 5.65 GHz, therefore the step size of frequency spectrum for the radiation characteristics measurement is chosen to be 0.05 GHz.

B.2.2 Procedure

The following explains the procedure for the test:

1. Measure known antenna (*MVG SH800*) with known radiation characteristics.
Use for gain reference.
2. Secure DUT to test platform.
3. Perform automated test by activating the measurement equipment of the chamber.

Since the antenna is not designed for use below 4 GHz, this is set as the start frequency. The measurement equipment cannot measure above 6 GHz, therefore this is the end frequency. The *StarMIMO* measures at angle steps of 15° in both planes.

B.2.3 Result

The data collected is imported into *Matlab* for visualization. The figure B.2 shows the elevation plane of the measured horn antenna in the anechoic chamber. The red line shows the radiation pattern for the horn antenna at $f = 4.75$ GHz. The blue line shows the radiation pattern for the horn antenna at $f = 5.65$ GHz. The antenna has a higher gain at $f = 5.65$ GHz of 12.99 dB, whereas at $f = 4.75$ GHz the highest gain is 11.41 dB. The 3 dB-bandwidths are also plotted at 19° for $f = 5.65$ GHz and at 22.5° for $f = 4.75$ GHz. For this reason, the chosen angle step for the measurements with the turntable is 20°.

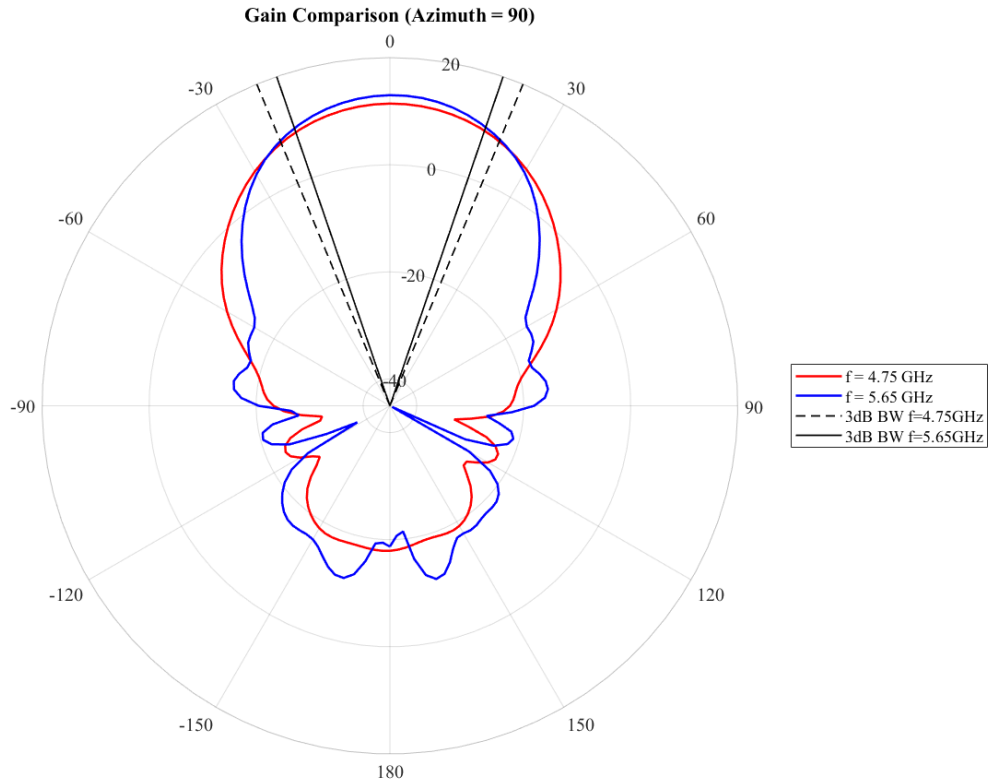


Figure B.2: Measured gain in the farfield at 4.75 GHz and 5.65 GHz (elevation plane).

Figure B.3 shows the azimuth plane of the horn antenna as measured in the anechoic chamber. The red line shows the gain for the antenna at $f = 4.75\text{ GHz}$ and the blue line shows the gain for the antenna at $f = 5.65\text{ GHz}$. The maximum gain is 12.99 dB at 0° .

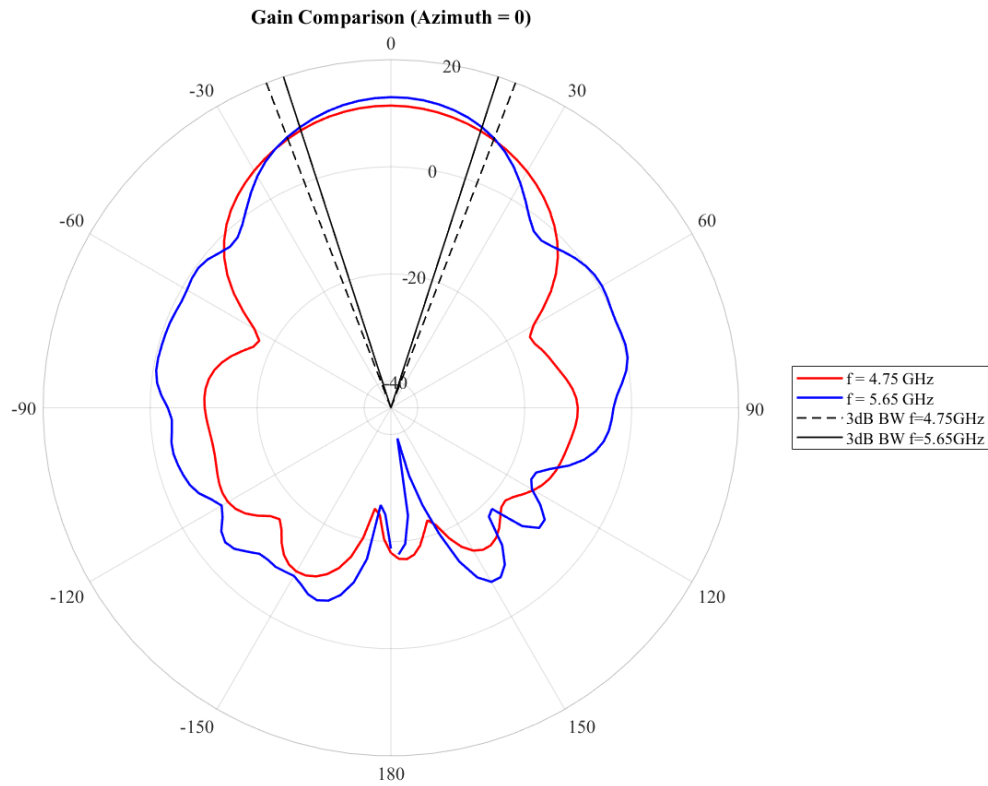


Figure B.3: Measured gain in the farfield at 4.75 GHz and 5.65 GHz (azimuth plane).

The evolution of the gain in the boresight direction as a function of frequency is plotted in figure B.4. The measurement shows that the gain, generally, increases as the frequency increases.

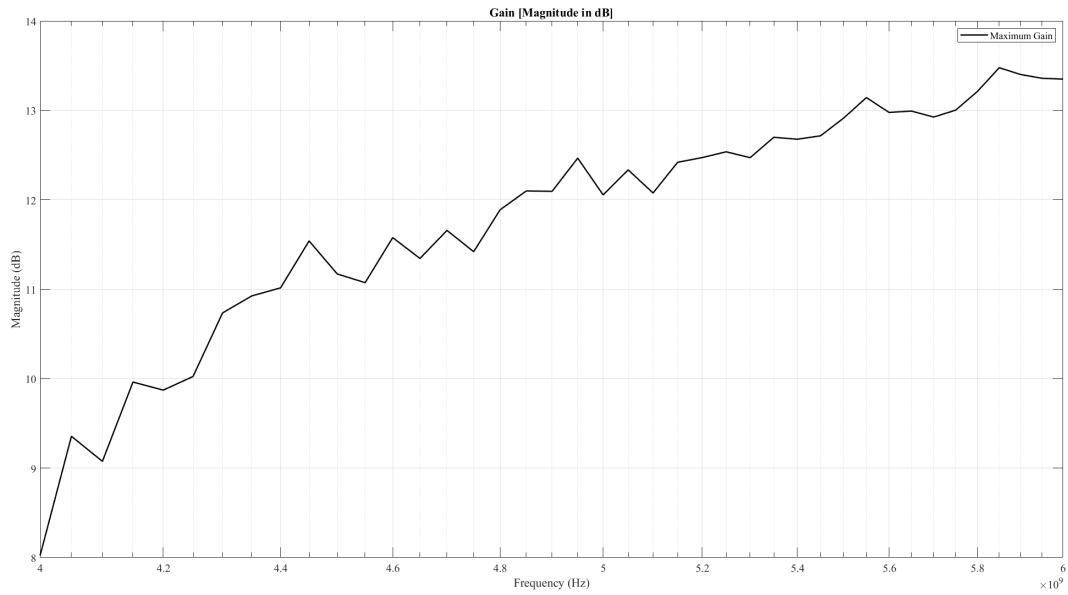


Figure B.4: Measured gain of horn antenna in the boresight direction in the frequency spectrum from 4 GHz to 6 GHz.